Oxidative dehydrogenation of ethane (ODHE) to ethylene by bulk MoVNbTe mixed oxide M1 phase catalysts

Applied Catalysis B: Environment and Energy 371 (2025) 125194

Contents lists available at ScienceDirect

Applied Catalysis B: Environment and Energy

journal homepage: www.elsevier.com/locate/apcatb

Oxidative dehydrogenation of ethane (ODHE) to ethylene by bulk MoVNbTe mixed oxide M1 phase catalysts

Dang D. Nguyen [a,1,2], Bar Mosevitzky Lis [a,b,1,3], Israel E. Wachs [a,*,4]

[a] Operando Molecular Spectroscopy and Catalysis Laboratory, Department of Chemical and Biomolecular Engineering, Lehigh University, Bethlehem, PA 18015, USA

[b] Department of Chemical Sciences and Bernal Institute, University of Limerick, Limerick, V94 T9PX, Ireland

ARTICLE INFO

Keywords:
Oxidative dehydrogenation of ethane
Bulk MoVNbTe
Raman
XRD
LEIS
XPS
SEM
TEM

ABSTRACT

The conversion of ethane to ethylene by steam cracking is an energy-intensive process that also produces significant global warming CO_2 emissions. An alternative process that is not as energy-intensive and produces significantly less CO_2 emissions is the oxidative dehydrogenation of ethane to ethylene by the bulk MoVNbTe mixed oxide catalyst. This paper reviews the current understanding of this catalytic reaction system to determine the nature of the bulk and surface phases of this important catalytic reaction. Although the crystalline M1 phase represents the bulk active phase, much is still unknown about the catalytic active surface sites of the M1 phase under reaction conditions. This review extensively examines the reported studies to date and outlines the experiments still needed to establish a fundamental structure-activity/selectivity relationship for this catalytic system that will guide the development of improved catalysts.

1. Introduction

Ethylene has become one of the most essential building blocks in the petrochemical industry [1,2] since its discovery over three centuries ago [3]. Both the global production and market size of ethylene have been on the rise and will keep increasing as the most produced petrochemical feedstock [4–9]. America and China have dominated the global ethylene production, and the worldwide market has been growing at ~3 % per year [1,6]. About 80 % of the produced ethylene is utilized in the manufacturing of commercially essential chemicals [1] (intermediate polymers (polyethylene, polystyrene, polyvinylchloride) [9–11], functionalized hydrocarbons (ethylene glycol, acetaldehyde, ethanol, dichloroethane) [1,2,12], higher olefins and liquid fuels [12–14], and many other products [15–17]).

Conventionally, steam cracking of ethane has been widely employed to produce ethylene [1,13,18,19]. However, this process requires an elevated operational temperature (~900 °C) due to the endothermic nature of ethane dehydrogenation [13,20–22]. As a result, steam cracking is susceptible to deactivation by coking of the reactor tubes [1,18,20] and significant emission of greenhouse gases [18,20,23]. The amount of ethane utilized in America to produce ethylene has increased more than two-fold since 2010 due to the growth of shale-based natural gas [24–27] and is projected to further expand by ~40 % by 2030 [24,26–29]. In order to meet the future production demands for ethylene, the oxidative dehydrogenation of ethane (ODHE) presents several competitive advantages over traditional ethane dehydrogenation. These include lowered thermodynamic barrier (less energy intensive) [13,30–36], minimized coke formation [37–39], reduced environmental impact [30,37–39], and alignment with several of the United Nation's 2030 sustainable development goals [40]. These goals include ensuring a healthy living environment against hazardous chemicals and air pollution (goal 3), promoting advancements in clean and energy-efficient technologies (goal 7), and combating climate change and its adverse impacts on society (goal 13).

From an industrial perspective, realistic commercialization of ODHE reaction requires the ethane conversion higher than 65 % [38,41], which is higher than the typical steam cracking process (Fig. 1), and the ethylene yield between 65 % and 70 % [41,42]. Many different types of catalysts have been proposed for the ODHE reaction since the first ODHE publication [43]: supported vanadium oxides [30,44,45], supported

* Corresponding author.
E-mail address: iew0@lehigh.edu (I.E. Wachs).
[1] Dang D. Nguyen and Bar Mosevitzky Lis contributed equally to this work
[2] 0009–0005-2959–4820
[3] 0000–0001-5793–5358
[4] 0000–0001-5282–128X

https://doi.org/10.1016/j.apcatb.2025.125194
Received 23 October 2024; Received in revised form 6 February 2025; Accepted 20 February 2025
Available online 28 February 2025

molybdenum oxides [46–48], bulk mixed metal oxides [38,49–53], supported nickel and cobalt oxides [54–56], supported alkali oxides and alkali chlorides [57–59]; supported rare earth metal oxides [60–62]; and other combinations [63–65]. Gaffney *et al.* have compared different ODHE catalysts and showed that, among these catalysts, the bulk M1 phase of the crystalline MoVNbTe mixed oxide catalyst possessed impressive ODHE catalytic performance in terms of high ethylene selectivity and good ethane conversions [66]. Fig. 1 demonstrates some of the best-performing catalysts and compares them with a typical steam cracker's catalytic data. At C_2H_6 conversions lower than 60 %, the bulk phase of MoVNbTe mixed oxide catalyst exhibits high selectivity to ethylene (more than 90 %), but this tends to drop slightly as ethane conversion increases. The negative correlation between ethane conversion and ethylene selectivity presents challenges for future studies since the industrial level of commercialization requires high ethane conversion (>65 %).

Most reported ODHE studies have characterized the bulk M1 phase under ambient conditions using bulk- and surface-sensitive techniques. Only limited *in situ* and *operando* spectroscopy information under ODHE operating conditions has been reported, which hinders efforts to establish structure-activity/selectivity relationships of the complex bulk M1 phase for the ODHE reaction. Furthermore, most of the research studies focused on propane (amm)oxidation to acrylonitrile and acrylic acid that was confirmed to have distinctive catalytic properties different from ODHE (e.g., activation energy, pre-exponential factor, rate constant, optimal operating temperature range, selectivity of the desired product) [13,31,82–84]. Consequently, the literature findings from propane oxidation are not directly transferable to ODHE. This paper summarizes and critically analyzes the progress of the bulk MoVNbTe mixed oxide (M1 phase) catalysts for ODHE. The findings reveal that much of the fundamental understanding of the bulk MoVNbTe mixed oxide M1 phase catalyst, bulk and surface phases, is still unknown [32,85] and the determination of the dynamics of the catalytic active sites is critical to guide the rational design of the bulk MoVNbTe mixed oxide (M1) catalyst.

2. Current understanding of the M1 phase of MoVNbTe mixed oxide system

2.1. Synthesis and crystalline bulk structure

The slurry method (SL) [69,73,84,86–97] and hydrothermal method (HT) [53,74–77,79,80,92,97–113] are the preferred approaches to synthesize the bulk MoVNbTe mixed oxide catalysts. The mixing procedure, drying method, and calcination conditions significantly impact the bulk and surface structures of MoVNbTe mixed oxide catalysts [114]. The final pH of the slurry also influences the formation of the crystalline phases after heat treatment [115]. Regarding the precursors for V incorporation, ammonium metavanadate was preferred for the SL [84,94–96] while vanadyl sulfate was preferred for the HT [76,77,92, 102–104,107,112,113]. During the SL, after the precipitation or evaporation of water from the aqueous mother liquor, calcination in air and subsequent annealing under an inert environment resulted in MoVNbTe mixed oxide catalysts with several desired (crystalline M1) and undesired phases (crystalline M2 and other bulk phases) [84,95]. The HT is superior to the SL since it promotes interactions among the metal ions and facilitates rapid formation of the desired crystalline structure (e.g., the crystalline M1 phase) [74,101,110]. In some instances, preparation of the M1 phase by HT was reported to yield catalysts with an order of magnitude higher surface area of ~50 m^2/g [74,99,106,109], which was attributed to the effect of oxalic acid post-treatment following the hydrothermal synthesis step [74,99]. Generally, the literature has concurred with the importance of including oxalic acid before [92,106, 109] or after [74,99] the autoclave treatment to obtain the bulk catalysts with higher surface area. Otherwise, the bulk MoVNbTe mixed oxide catalysts synthesized by the conventional SL [73,86,88,90–92] and the oxalic acid-free HT [53,74,75,87,89,92,98,100,102] possess low surface areas (<30 m^2/g), which limits the types of characterization instruments that can be used for their investigation.

The synthesized bulk MoVNbTe mixed oxide catalysts contain two main bulk crystalline structures, M1 and M2 phases, and other secondary bulk crystalline phases: V/Nb-substituted Mo_5O_{14} [52,53,68,74,116, 117], MoO_3 [103,118,119], $TeMo_5O_{16}$ [53,94,103,116,118–122], and even metallic Te after extended operation [71,74,123]. The morphology of the M1 crystals consists of flattened [124] and needle-like [96,124] particles having channels that are 0.4–0.6 nm in diameter [117,124].

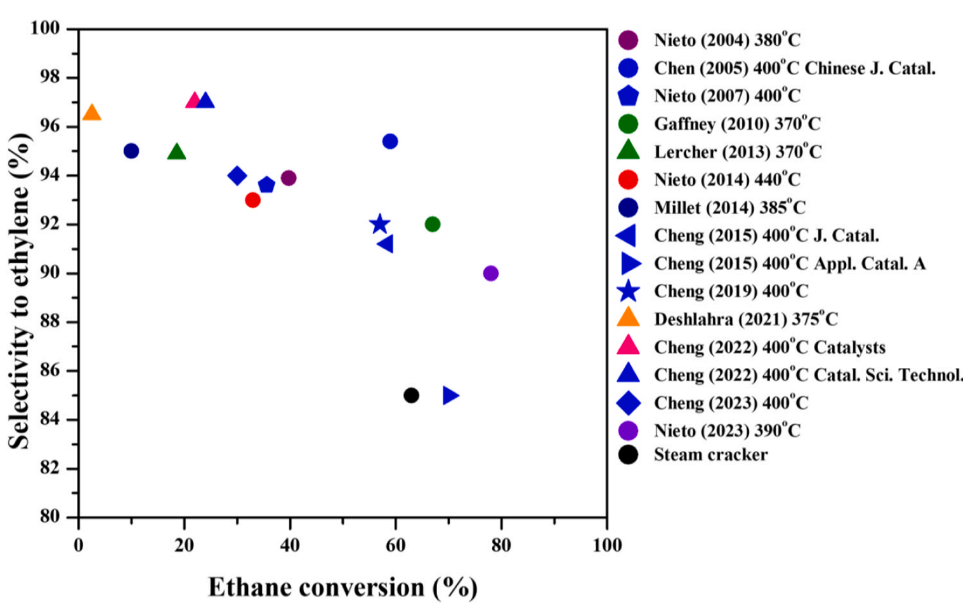

Fig. 1. Comparison of catalytic performance of ethane steam cracker (hydrogen, methane, heavier hydrocarbons as byproducts) and the literature-reported best-performing bulk MoVNbTe mixed oxide catalyst, which are heated-treated at 600 °C under inert gas, for ODHE in terms of ethane conversion and ethylene selectivity, constructed from literature data points [67–81]. The data points are color-coded, reflecting different operating temperatures.

The crystalline bulk structure of the (001) facet of the M1 phase is shown in Fig. 2 [124]. The orthorhombic M1 phase (Pba2), which has the formula $Te_2M_{20}O_{57}$ (M = Mo, V, Nb), consists of pentagonal rings connected by corner-sharing MO_6 octahedrons (M = Mo, V) to form hexagonal and heptagonal rings with the Te-O units [68,116,120,124–129]. The hexagonal and heptagonal channels have pore diameters of 0.47 nm and 0.58 nm, respectively [69]. The Nb^{5+} atoms preferentially occupy the pentagonal rings (S9 sites) and are surrounded by a combination of Mo^{6+} and V^{5+} atoms [102,116,130]. The hexagonal and heptagonal rings are composed of assorted $Mo^{5+/6+}$ and $V^{4+/5+}$ atoms surrounding a single Te^{4+} atom (S12 and S13 sites) [124,128,129]. Recent studies have shown that vanadium atoms preferentially occupy the following bulk sites in the order: S2 > S3 > S7 > S4 ≈ S1 [117,131–133].

The bulk M2 phase (Pmm2) can also be present, which corresponds to $Te_{0.33}MO_{3.33}$ (M=Mo, V, Nb), and is composed of pseudo-hexagonal rings hosting Te-O units without any pentagonal or heptagonal rings [116,117,120,126–129] as illustrated in Fig. 3. Two structural features differentiating the M2 phase from the M1 phase are the lack of the pentagonal bipyramidal structure whose center contains an Nb^{5+} atom [102] and the absence of the V^{5+} centers [120] in the M2 bulk structure. The performance of the bulk MoVNbTe mixed oxide catalyst was initially proposed to be associated with the presence of the M2 and metal-substituted Mo_5O_{14} phases [41,52,53,68], even though these species only exist as minor components in the highly active catalysts. Subsequently, the M1 phase was shown to be the most probable source of catalytic activity [41,52,66,68,69,86,89,102,117,120,134,135]. Therefore, the pure bulk M1 phase is preferably obtained from hydrogen peroxide and oxalic acid treatments to remove the M2 phase and other secondary metal oxide phases [74,135–137]. Later studies have found post-treatment with nitric acid to be sufficient for the purification of the M1 phase in the synthesized bulk catalyst [77,79,80,138] due to concern with the loss of surface vanadium by oxalic acid treatment [74].

2.2. Bulk spectroscopic characterization

Details of the bulk electronic structures and local symmetries associated with the molecular orbital energies and occupancies are accessible with X-ray Absorption Near-Edge Spectroscopy (XANES). The bulk oxidation states of the MoVNbTe mixed oxide catalysts, prepared by both SL and HT, have been determined using XANES, but not under ODHE reaction conditions [94,122,130,139–141]. The *ex situ* XANES data under ambient conditions revealed that the bulk M1 phase (HT) contains Nb^{5+}, Te^{4+}, Mo^{6+}, and V^{4+} [130,140]. Confirmation of the presence of V^{4+} in the bulk MoVNbTe mixed oxide catalysts is with complementary Electron Paramagnetic Resonance (EPR) studies of both SL and HT catalysts [92,139]. Several *ex situ* XANES studies suggested

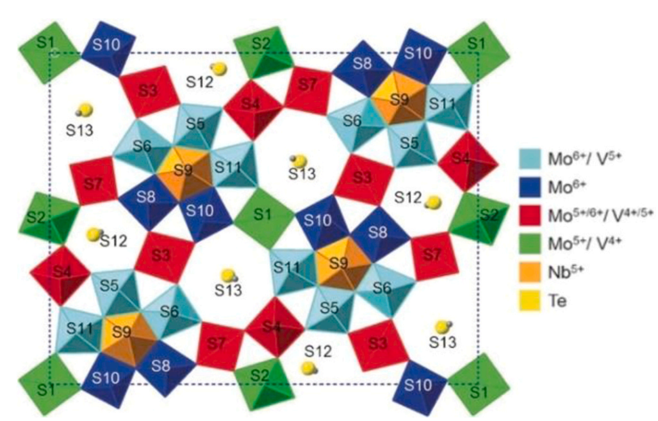

Fig. 2. Crystalline bulk structure of the (001) facet of the M1 phase [124]. Adapted with permission from reference [124]. Copyright 2016 John Wiley and Sons.

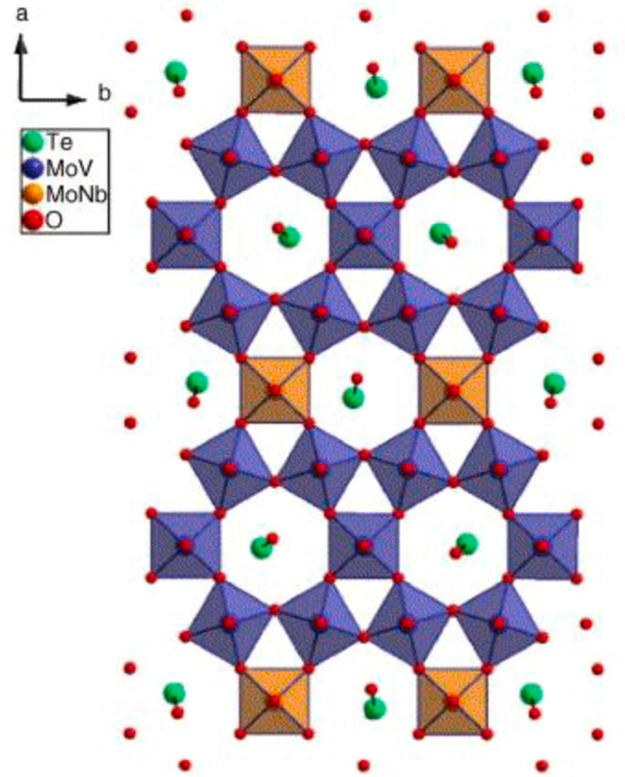

Fig. 3. Schematic representation of the refined structural models of the bulk M2 phase ($Mo_{4.31}V_{1.36}Nb_{0.33}Te_{1.81}O_{19.81}$) as 2 × 2 unit cell model [95]. Adapted with permission from reference [95]. Copyright 2006 Elsevier.

that the average valence state of V in the M1 phase (SL and HT) is 4 + and accompanied by a small fraction of V^{5+} [122,130,139]. Furthermore, XANES results of SL and HT bulk catalysts demonstrated that only a small fraction of the bulk Mo^{6+}, V^{4+}, and Te^{4+} cations undergo redox under oxidative (O_2) and reducing (H_2) conditions [130, 139–141]. Comparing the XAS absorption edges of the bulk M1 phase (HT) and the Nb_2O_5 reference (Nb^{5+}), the valence state of Nb was found to remain at the highest oxidation state of 5 + upon switching between 10 % O_2/He (oxidative) and 4 % H_2/He (reducing) environments [140], suggesting it may not readily undergo redox. *In situ* XANES studies of the bulk M1 phase are only available under propane oxidation reaction conditions, not ODHE.

The HT bulk M1 structure is preserved, before and after heating at 400 °C under 0.9 mbar ethane oxidation (C_2H_6/O_2/He = 30 %/20 %/50 %) reaction conditions [123], as observed with Environmental Scanning Transmission Electron Microscopy (ESTEM). A High-Angle Annular Dark-Field (HAADF) STEM study of the Nb-free HT bulk MoVTe mixed oxide catalyst found that the bulk M1 structure, despite the absence of Nb cations, maintained its bulk structural integrity under various environmental conditions (including ultra-high vacuum (UHV), reduction by C_2H_6, and 1 mbar under a propane reaction mixture (O_2/C_3H_8/He = 30 %/15 %/55 %) [142]. Although these studies have shown the M1 bulk structure to be relatively stable, the complex dynamic catalyst changes at the atomic level and the thin surface active layer (~1nm) model cannot be dismissed.

X-ray Diffraction (XRD) has been extensively used to detect the contributions from various crystalline phases present in the bulk MoVNbTe structure, but only under ambient conditions [52,53,67–69, 71,73–75,78,81,84,86,88–107,109–112,114–119,121,122,124–127, 130,132,134–166]. The bulk M1 phase (ICSD 55097, PDF 00–058–0789) has XRD diffraction lines at 2θ = 6.6°, 7.7°, 8.9°, 22.1°, and 27.1°, while the XRD peaks of the bulk M2 phase (ICSD 55098, PDF

00–057–1099) are located at 2θ = 22.1°, 28.1° and 36.2° [74,75,78,81,91,98,99,101,138,147,156,166]. An *in situ* XRD study by Svintsitskiy *et al.* examined a SL bulk M1 phase [167] under an ethane-reducing environment (C_2H_6/He = 8 %/92 %), revealing initial degradation of this M1 bulk structure, indicating the formation of the bulk MoO_2 phase (Mo^{4+}), starting from 520 °C to complete disintegration at 560 °C. Although XRD is an excellent tool to characterize the crystalline phases present in the bulk MoVNbTe mixed oxide catalysts, their surface dynamics can only be obtained through surface-sensitive techniques (see Section 2.3).

Raman is a complementary characterization tool to XRD to probe the presence of crystalline V_2O_5, MoO_3, TeO_2, and Nb_2O_5 nanoparticles given Raman's strong sensitivity to these crystalline metal oxide phases. The bulk M1 phases prepared by both SL [69,71,84,95,144–146,168] and HT [81,87,102,126,138,147,148,169] have been examined with Raman spectroscopy. However, *in situ* Raman measurements under ODHE are not readily available. For example, the *in situ* Raman spectra for the bulk MoVNbTe mixed oxide catalyst prepared by HT appear in Fig. 4. The Raman spectra of the bulk binary $M_{0.6}V_{1.5}O_x$ (black line) and bulk MoO_3 (blue line) are compared in Fig. 4, indicating that the structure of the bulk $M_{0.6}V_{1.5}O_x$ resembles a distorted MoO_3 structure, as evidenced by the Raman bands at 865 cm^{-1} and 980 cm^{-1} instead of 812 cm^{-1} and 993 cm^{-1}, respectively. The higher vibrational contribution of bulk molybdena phase than bulk vanadia phase to the Raman spectrum of the bulk $Mo_{0.6}V_{1.5}O_x$ phase is related to the more prominent Raman scattering cross-section of MoO_3 than V_2O_5 [87]. The Raman band at 865 cm^{-1} has been associated with asymmetric vibrations of the bridging Mo-O-Mo and Mo-O-V stretching modes [69,81,84,87,138] and the shoulder band at 980 cm^{-1} has been assigned to the vibrations of terminal Mo═O and V═O stretching modes [69,81,87,126,138]. Upon increasing the Mo/V ratio (black line to red and green lines in Fig. 4), however, a reduction in the relative Raman intensity of the 980 cm^{-1} vibration was observed [87], indicating that this band is possibly associated with V═O vibrations. As the Mo/V ratios were increased for the corresponding bulk tertiary $Mo_1V_{0.5}Te_{0.16}O_x$ (red line in Fig. 4) and quaternary $Mo_1V_{0.3}Te_{0.16}Nb_{0.12}O_x$ (green line in Fig. 4) catalysts, their Raman spectra did not experience a significant change compared to that of the bulk binary catalyst. This is due to the overwhelming Raman scattering cross-section of the Mo-O vibrations and the analogous bulk molybdenum oxide structures present in these catalysts. The additional 910 cm^{-1} shoulder band in the Raman spectrum of the bulk $Mo_1V_{0.5}Te_{0.16}O_x$ catalyst, compared to that of the bulk $M_{0.6}V_{1.5}O_x$ catalyst, is associated with the incorporation of Te cations into the catalyst's framework [95,149]. A weak shoulder at ~800 cm^{-1} was present in the Raman spectrum of the bulk quaternary $Mo_1V_{0.3}Te_{0.16}Nb_{0.12}O_x$, unlike those of bulk $Mo_{0.6}V_{1.5}O_x$ and bulk $Mo_1V_{0.5}Te_{0.16}O_x$ that can be associated with a trace amount of MoO_3 nanoparticles, given the sharp band of crystalline MoO_3 nanoparticles at 812 cm^{-1}. The absence of sharp Raman bands from separate crystalline V_2O_5, TeO_2, and Nb_2O_5 phases [87,95,150] in the Raman spectrum of bulk $Mo_1V_{0.3}Te_{0.16}Nb_{0.12}O_x$ confirms the incorporation of these metal oxides into the catalyst bulk mixed oxide structure.

Most of the reported Raman spectra from the bulk MoVNbTe mixed oxide catalysts correspond to ambient conditions. The bulk MoVNbTe mixed oxide catalysts synthesized by the SL [69,71,84,146] and HT [81,102,126,138,147,148] procedures exhibit the same Raman spectrum: an intense band at ~875–880 cm^{-1} coupled with two weaker shoulder bands at ~800–820 cm^{-1} and 980 cm^{-1}. Comparison between the ambient Raman spectra of the bulk M1 and M2 phases [69] revealed that these bulk structures are indiscernible using only vibrational Raman spectroscopy. Consequently, it is necessary to collect both the Raman and XRD spectra to confirm if both of these phases co-exist in the structure of the bulk $MoVNbTeO_x$ catalyst. *In situ* Raman measurements under propane oxidation reaction conditions (C_3H_8/O_2 = 6/1–1/1) demonstrated the bulk stability of the quaternary $Mo_{1.0}V_{0.3}Te_{0.16}Nb_{0.12}O_x$ catalyst under propane reactive environments where there is no overall increase in the oxidation state [87]. Despite the current progress, *in situ* and *operando* Raman data under ODHE conditions for MoVNbTe mixed oxide in the literature are still rare, and the relationships between the crystalline MoO_3 and V_2O_5 nanoparticles and ODHE activity also require further investigation.

2.3. Surface spectroscopic characterization

Low-Energy Ion Scattering (LEIS) spectroscopy monitors the elemental composition of the outermost surface atoms (~0.3 nm) and the depth profile of atoms below the outermost surface when combined with sputtering, but requires an UHV environment. Guliants *et al.*

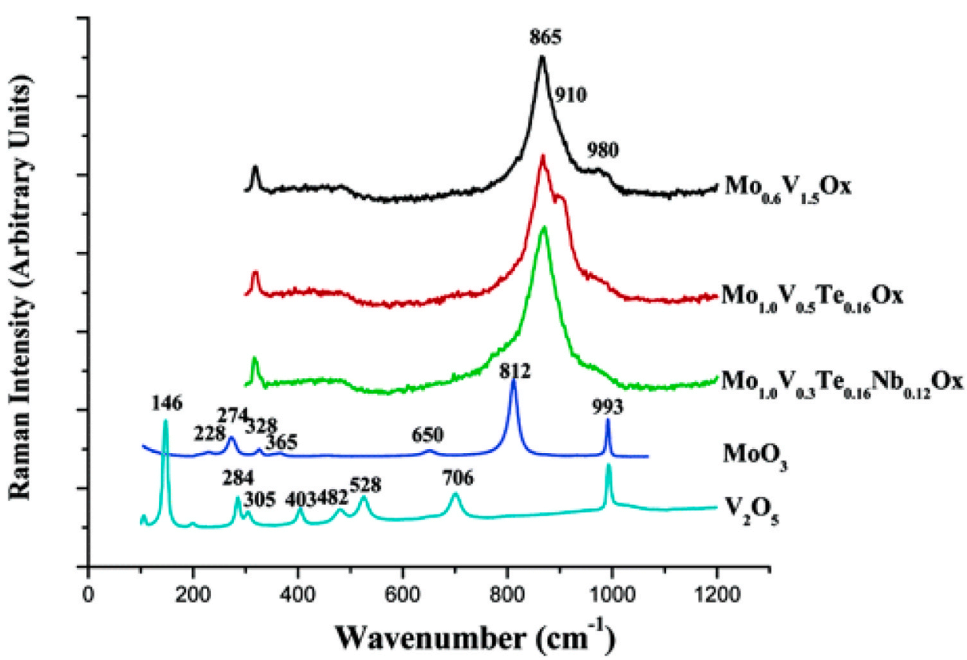

Fig. 4. *In situ* Raman spectra of bulk $Mo_{0.6}V_{1.5}O_x$, $Mo_{1.0}V_{0.5}Te_{0.16}O_x$, $Mo_{1.0}V_{0.3}Te_{0.16}Nb_{0.12}O_x$ under dehydrated conditions at 350°C. The Raman spectra of the bulk MoO_3 and V_2O_5 metal oxides are included for reference [87]. Adapted with permission from reference [87]. Copyright 2005 American Chemical Society.

reported High Sensitivity-LEIS (HS-LEIS) data showing the depletion of V (-23 %) and Mo (-27 %) and the enrichment of Te (+165 %) and Nb (+55 %) in the outermost surface layer of their HT bulk MoVNbTe mixed oxide catalyst [151,152]. The elemental composition of the topmost surface layer remained relatively the same before and after heat treatment at 400 °C under UHV. Sanfiz *et al.* conducted a High-sensitivity LEIS (HS-LEIS) experiment under UHV to examine their SL bulk MoVNbTe mixed oxide catalyst [153]. The surface composition of the catalyst changed after exposure of the SL catalyst to propane oxidation: Te was surface-enriched, V was surface-depleted, and the surface Mo and Nb concentrations remained the same as in the bulk phase [153].

The comparison of reported bulk and surface compositions of the bulk MoVNbTe mixed oxide catalysts from the literature appears in Table 1. The XPS analyses of the surface region (~1–3 nm) of the crystalline MoVNbTe (M1 phase) synthesized using SL [135,139] and HT [74,78,98,99,118] under UHV conditions show that mixtures of V^{5+}/V^{4+} and Te^{6+}/Te^{4+} oxidation states were present in these bulk catalysts [74,78,98,99,118,135,139]. The percentages of surface V^{5+} over total surface vanadium contents were quantified by UHV XPS to vary from 22.5 % to 65.8 % [73,75,78,98,99,118]. Meanwhile, one XPS study showed that surface Te^{4+} accounted for the majority (65.4 %) of total tellurium present on the surface under UHV conditions [99]. Other XPS studies under UHV environments also reported detecting mixtures of Mo^{5+}/Mo^{6+} [135,139,154]. Specifically, a small fraction of surface molybdenum (6–12 %) was shown to exist in the reduced state (Mo^{5+}) [135,139,154]. Surface niobium was present as Nb^{5+} in all UHV XPS studies. Comparison of the EDS/ICP bulk and UHV XPS surface compositions revealed that V is depleted in the surface region relative to Mo [68,73–75,86,98,118,126,135,139,141,154]. Contradictory data have been reported about surface enrichment/depletion of Te and Nb in comparison to Mo, with more frequent reports of surface-enriched Te and Nb concentrations [43,68,74,75,98,118,126,135,139,154]. The above XPS studies, however, employed UHV conditions where surface cations can be reduced by stimulation of the exciting X-rays and ejecting electrons [170] that should minimize under reactive environments [171]. Thus, the interpretation of XPS measurements collected under UHV conditions requires extreme care.

The development of Near-Ambient Pressure XPS (NAP-XPS) has allowed researchers to close the gap between UHV and reaction conditions. The dynamic nature of the surfaces of mixed metal oxides emphasizes the importance of performing surface analysis of the bulk M1 phase with NAP-XPS under ODHE conditions. In an *in situ* NAP-XPS study under several ODHE environments (molar gas ratio C_2H_6/O_2 = 1–10/1) at 400 and 460 °C, Ishchenko *et al.* investigated a SL bulk MoVNbTe mixed oxide catalyst with an M1 crystallinity degree of 74 % [167] and demonstrated V was surface depleted, while Nb and Te were surface enriched at ~1.8 nm depth [167]. Additionally, upon transition from UHV to ODHE conditions (Fig. 5), a small amount of Mo^{6+} (6 % of total Mo) and V^{5+} (7 % of total V) species were reduced to Mo^{5+} and V^{4+}, respectively, under the ODHE reaction (molar gas ratio C_2H_6/O_2 = 1/1) conditions [167]. The oxidation states of the Nb^{5+} and Te^{4+} cations remain fully oxidized (Nb^{5+} and Te^{4+}, respectively) under the ODHE

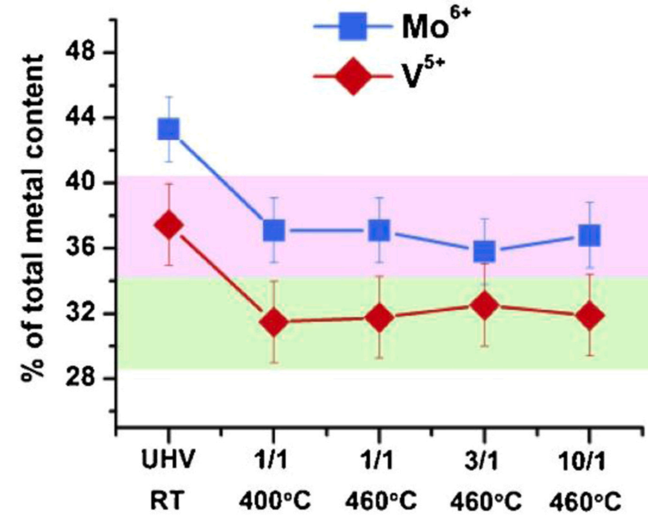

Fig. 5. Mo^{6+} and V^{5+} fractions, with respect to total Mo and V, on the outermost surface layer of a bulk MoVNbTe catalyst under different environmental conditions: UHV RT (~10^{-9} mbar and room temperature) and other reaction conditions (1 mbar and 400 or 460 °C). The feed C_2H_6/O_2 ratio varied from 1/1–10/1 [167]. Adapted with permission from reference [167]. Copyright 2019 Elsevier.

Table 1
Bulk compositions as measured by Energy Dispersive X-ray Spectroscopy (EDS) or Inductively Coupled Plasma (ICP) and surface compositions as measured by UHV XPS for the bulk MoVNbTe mixed oxide catalysts. All catalysts calcined under inert atmospheres (Ar or N_2) at 600 °C for 2 hr.

Bulk composition (EDS or ICP) Mo/V/Nb/Te	Surface composition (UHV XPS) Mo/V/Nb/Te	Synthesis method	Mo oxidation states	V oxidation states	Nb oxidation states	Te oxidation states	Reference
1/0.14/0.17/0.19	1/0.11/0.22/0.19	HT	-	-	-	-	[68]
1/0.39/0.17/0.16	1/0.31/0.10/0.16	HT	-	-	-	-	[68]
1/0.23/0.14/0.13	1/0.14/0.14/0.10	SL	+ 6	+ 4,+ 5	+ 5	+ 4	[73]
1/0.26/0.13/0.09	1/0.18/0.12/0.09	SL	+ 6	+ 4,+ 5	+ 5	+ 4	[73]
1/0.21/0.19/0.22	1/0.13/0.17/0.29	HT	+ 6	+ 4,+ 5	+ 5	+ 4,+ 6	[74]
1/0.16/0.30/0.09	1/0.11/0.38/0.11	HT	+ 6	+ 4,+ 5	+ 5	+ 4,+ 6	[74]
1/0.19/0.23/0.08	1/0.10/0.29/0.11	HT	+ 6	+ 4,+ 5	+ 5	+ 4	[75]
1/0.19/0.25/0.09	-	HT	+ 6	+ 4,+ 5	+ 5	+ 4,+ 6	[78]
1/0.25/0.24/0.12	1/0.10/0.34/0.21	HT	+ 6	+ 4,+ 5	+ 5	+ 4	[79]
1/0.22/0.23/0.26	1/0.14/0.28/0.40	HT	+ 6	+ 4,+ 5	+ 5	+ 4	[81]
1/0.21/0.09/0.22	1/0.12/0.29/0.10	HT	+ 6	+ 4,+ 5	+ 5	+ 4,+ 6	[98]
1/0.12/0.36/0.12	-	HT	+ 6	+ 4,+ 5	+ 5	+ 4,+ 6	[99]
1/0.22/0.23/0.26	1/0.10/0.25/0.29	HT	+ 6	+ 4,+ 5	+ 5	+ 4	[118]
1/0.25/0.37/0.27	1/0.13/0.21/0.60	HT	+ 6	+ 5	+ 5	+ 4	[126]
1/0.29/0.37/0.27	1/0.14/0.24/0.53	HT	+ 6	+ 5	+ 5	+ 4	[126]
1/0.31/0.39/0.38	1/0.19/0.15/0.39	HT	+ 6	+ 5	+ 5	+ 4	[126]
1/0.28/0.37/0.27	1/0.15/0.24/0.56	HT	+ 6	+ 5	+ 5	+ 4	[126]
1/0.32/0.38/0.28	1/0.16/0.24/0.48	HT	+ 6	+ 5	+ 5	+ 4	[126]
1/0.32/0.35/0.25	1/0.16/0.18/0.45	HT	+ 6	+ 5	+ 5	+ 4	[126]
1/0.26/0.12/0.11	1/0.14/0.14/0.13	SL	+ 5,+ 6	+ 4	+ 5	+ 4,+ 6	[135]
1/0.26/0.15/0.09	1/0.16/0.14/0.30	SL	+ 5,+ 6	+ 4	+ 5	+ 4,+ 6	[139]
1/0.23/0.14/0.13	1/0.14/-/0.10	SL	+ 6	+ 4,+ 5	+ 5	+ 4	[141]
1/0.25/0.12/0.11	1/0.18/0.17/0.19	HT	+ 5,+ 6	+ 4	+ 5	-	[154]

environments [167]. The currently reported NAP-XPS studies agree on the reduction of the V and Mo cations in the surface region of bulk MoVNbTe mixed oxide catalysts for ODHE, notably the apparent reduction of Mo^{6+} to Mo^{5+} under ODHE conditions [167] that requires more experimental studies to confirm.

The above NAP-XPS and LEIS studies demonstrate that the elemental surface composition and cation oxidation states of the unsupported bulk MoVNbTe mixed oxide are dynamic and dependent on environmental conditions requiring systematic investigations. The demanding reaction conditions for ODHE [13,31,83,172,173] are expected to result in a unique surface state of the dynamic bulk MoVNbTe mixed oxide catalysts. Obtaining a comprehensive understanding of the dynamics of the bulk MoVNbTe mixed oxide catalysts during ODHE requires additional *in situ* and *operando* surface spectroscopic studies.

2.4. ODHE Reaction kinetics

Valente *et al.* investigated the kinetics for ODHE by the SL bulk M1 phase catalyst and found that the reaction was highly sensitive to ethane partial pressure with reaction orders of 1.5 for ethylene formation and 1.33–1.8 for CO_x production [156]. In contrast, the O_2 partial pressure had a minimal effect on the formation of all products, exhibiting reaction orders of 0.13 for ethylene formation and 0.3 for CO_x production [156]. Subsequent result showed agreement with minimal impact of oxygen partial pressure on reaction rates [174]. The weak dependence of ODHE on the partial pressure of molecular O_2 suggested a Mars-van Krevelen mechanism involving the participation of the lattice oxygen from the M1 phase and that the surface active sites are present as moderately oxidized during the ODHE reaction. Kinetic studies have attempted to fit the surface reaction mechanism by suggesting that both CO and CO_2 byproducts derive from ethane oxidation during ODHE, and the formation of CO from ethylene only occurs in modest amounts [156]. The calculated kinetic parameters showed that the overall oxidation of ethane to ethylene had the lowest activation energy (119 kJ mol^{-1}), while the competing oxidation reactions of ethane to CO_x exhibited higher activation energies, 143 and 217 kJ mol^{-1} for reactions from ethane oxidation to CO and CO_2, respectively [156]. The higher activation energies of the progressive oxidation reactions to CO_x imply that an increase in reaction temperature favors the CO_x-produced reactions over the partial oxidation reaction of ethane to ethylene. Subsequent kinetic results from the same group [175], using the same SL bulk M1 phase catalyst, demonstrated that ethylene oxidation on bulk MoVNbTe to generate CO_2 did play a role in the reaction scheme with similar high activation energies of 190 and 177.8 kJ mol^{-1} for the reaction steps from ethylene to CO_2 and CO, respectively [175]. Later studies demonstrated that ethylene oxidation on MoVTeNb mixed oxide catalysts generates CO_2 (albeit 3–4 times less than CO), suggesting that the CO_2 formation stems from ethane oxidation, ethylene oxidation, CO oxidation, or a combination of the three [175,176]. CO_x poisoning, due to competitive re-adsorption of CO_x at the active site [1,175,176], has a low probability due to the known weak CO-metal oxide interaction.

The above ODHE and ethylene oxidation data were fitted to the overall surface reactions following the Langmuir-Hinshelwood, Eley-Rideal, and Mars-Van Krevelen mechanisms [175,176]. The fitted activation energies indicated that the formation of ethylene from ethane was the most energetically favorable reaction (reaction with the lowest activation energies) [175,176] and that the activation energies of the formation of CO_2 and CO from ethylene were lower than those from ethane regardless of the kinetic model [176,177]. The Langmuir-Hinshelwood mechanism achieved the best agreement among the proposed reaction mechanisms [175,176]. Simplifying assumptions, however, were required to untangle the dynamically complex reaction kinetics, which made it challenging to distinguish among the different macroscopic mechanistic approaches. The raw kinetic data plainly shows the relevance of the Mars-van Krevelen mechanism as described above. Still, by removing the complexities from the reaction kinetics, the Langmuir-Hinshelwood model became the most favorable.

Experimental clarification for the dominant surface reaction mechanism for ODHE by the bulk MoVNbTe mixed oxide catalysts has still not appeared in the literature. Vanadia-based catalysts are known to be one of the most active and selective catalysts for the ODH of light alkanes [30]. For model supported VO_x/Al_2O_3 and VO_x/ZrO_2 catalysts, isotopic labeling experiments indicated that C-H bond activation was the rate-determining step (RDS) [45]. This is relevant for the bulk MoVNbTe system since VO_x sites might participate directly as the main redox sites in the ODHE process. The activation energies of ethane's first C-H bond activation step were recently calculated with Density Functional Theory (DFT) calculations for several possible active sites: Te_{S12}=O (109 kJ mol^{-1}), V_{S7}=O (139 kJ mol^{-1}), and V_{S7}-O-Mo_{S4} (136 kJ mol^{-1}) that are shown in Fig. 2 [117]. These values are somewhat similar to the experimentally determined overall apparent activation energies for ODHE by the bulk M1 phase catalyst (77–115 kJ mol^{-1}) [117,175,176]. However, given the higher redox activity of the VO_x sites compared to TeO_x sites [87], the activation energies of V=O and V-O-Mo sites should have been lower than that of Te=O sites.

2.5. Catalytic reaction models based on bulk characterization

Early characterization studies of the bulk M1 mixed oxide phase only applied XRD and TEM under ambient conditions to determine the bulk crystalline structures and assumed that the outermost surface layer was just an extension of the bulk structure. For the ODHE reaction, ambient XRD and ambient TEM were employed to emphasize the importance of V/Nb-substituted the bulk Mo_5O_{14} phase for the highest-performance ODHE catalysts, hinting that the catalytic active sites are associated with the bulk structures [53,68]. Doping niobium (Nb) into bulk VMo mixed oxide catalysts improved performance and selectivity for ODHE at lower temperatures (300–400 °C) [43,157–160,178]. Botella *et al.* showed that the addition of Nb enhanced the surface area of the catalyst and prevented MoO_2 (Mo^{4+}) formation, proposing that this results in higher selectivity to ethylene [157]. It has been hypothesized, without supporting data, that the Te cation played an indirect role in ODHE, eliminating non-selective Mo-containing crystalline phases and facilitating the formation of the highly crystalline M1 phase [52,53,86]. For instance, the tellurium (Te)-containing bulk MoVNb mixed oxides exhibited significantly higher ethane conversion and selectivity to ethylene, ~95 % for one catalyst candidate, at 400 °C [52], which was attributed to the superior stability of the Te-containing catalyst during hydrothermal synthesis and the formation of the desired M1 phase [52,68,69,105]. XRD analysis of hydrothermally synthesized catalysts suggested that high crystallinity was crucial in achieving high ethane conversion and ethylene selectivity because of the superior catalytic performance of the orthorhombic bulk Mo_3VO_x phase over the other structures for ODHE [53,136]. There is no information at present, however, regarding the stability of the M1 phase under the ODHE reaction. It was also proposed that ethane ODH proceeds in the hexagonal channel of the M1 phase at the V^{5+} active site [86]. The literature has, in general, agreed on the importance of the Mars-van Krevelen mechanism based on the weak dependence of the reaction kinetics on the partial pressure of gaseous molecular O_2 [156]. However, there is still a great deal of uncertainty about the exact origin of the participating lattice O* , whether from the outermost surface layer (0.3 nm), the surface region (1–3 nm), the internal channel surface sites, or the crystalline bulk lattice.

2.6. Catalytic reaction models based on surface characterization

Obtaining surface data under reaction conditions is critical to the fundamental understanding of the bulk MoVNbTe mixed oxide catalytic system since the dynamics of the elemental concentrations in the near-surface region (~1–3 nm). The combination of bulk crystalline and surface data led to somewhat similar reaction models for both propane

ODH and ODHE reactions, but supporting data were not available under ODHE reaction conditions. The V^{5+}/V^{4+}, Mo^{6+}/Mo^{5+}, Te^{4+}, and Nb^{5+} cation sites are present in the near-surface region of unsupported MoVNbTe mixed oxide catalysts, as demonstrated by *in situ* NAP-XPS [98]. Several recent UHV XPS studies suggested that the V^{5+} cation in the near-surface region acts as the surface active site due to the correlation with the rate of ODHE oxidation [74,98]. Additionally, the role of the surface Mo^{6+}/Mo^{5+} mixture on the ODH of alkane has not been experimentally determined. It was proposed that the Te cation stabilizes the bulk crystalline M1 phase catalyst, without any supporting data [98]. A linear relationship between the rate of ethane conversion and the concentration of the catalyst's surface V^{5+} cation (NAP-XPS) has been demonstrated [98], further suggesting the role of V^{5+} in performing the first hydrogen abstraction step, which is the rate-determining step (RDS) in alkane oxidation [119,120]. This understanding heavily relied on previous knowledge of the crystalline M1 phase for propane ODH [116, 119,120], which might not apply to ODHE conditions.

The bulk M1 phase contains two surface candidates that are viable catalytic active sites: the external surface sites and the internal channel surface sites. The influence of internal and external surface sites of the crystalline M1 phase on the ODHE activity was also explored in both experiment [76,99,117,124] and theory [117,179]. DFT simulations suggested that, by stabilizing C_2H_6 molecules with van der Waals interactions, the M1 phase heptagonal channels perform C-H activation (RDS) [117]. Furthermore, the DFT calculations suggest that C-H activation and C-O formation steps require interactions with terminal oxygens located on the (001) plane [179]. This finding contradicts the highest activation energy of the V=O bond [117], considering the prevalent evidence of VO_x sites participating in the C-H cleavage step [74,86,98]. Comparing the activation energies between internal and external surface sites using two different molecules (C_2H_6 and C_6H_{12}) suggested the ODHE occurred on the internal heptagonal channels [76], under the assumption that C_2H_6 molecules enter both internal and external sites. However, the intrinsic rates of these molecules were shown not to be the same [76] and C_2H_6 molecules might only interact with the external surface sites. The use of various morphological samples of the M1 phase indicated that the (001) facet alone was not responsible for controlling the ODHE catalytic activity [124]. Growing thin M1 phase samples perpendicular to the (001) facet was shown to increase catalyst performance [99]. Adjusting the number of external surface sites and internal surface sites on the channel walls of the crystalline M1 phase, using oxalic acid treatment, suggested that the active sites located on the external surface were less active and selective for ODHE ($C_2H_6/O_2/He = 30\,\%/20\,\%/50\,\%$) than the surface sites inside the wall channels [99]. This observation presents an alternative perspective to the extensive literature supporting the existence of significant ODHE activity on the external surface of the M1 phase [99,117,124], despite the absence of direct supporting evidence. This surface could be at least partially amorphous, as supported by ADF-STEM and HAADF-STEM measurements indicating the prevalence of non-crystalline amorphous phases in MoVNbTe mixed oxide M1 phase catalysts [124,128,129]. These data indicate the possible existence of a thin amorphous overlayer on the crystalline M1 phase [91,117,124,129,162,163] and are supported by the different LEIS-determined surface compositions of MoVNbTe mixed oxide catalysts [151,162,164]. In summary, the catalytic active sites of the bulk M1 phase catalyst are proposed to be located within the pore channels of the crystalline M1 phase. It is also essential to note that the potential existence of the same catalytic active sites on the external surface needs to be considered because most of the literature studies have not distinguished between the inside and outside surface regions of the crystalline M1 phase. Consequently, further systematic fundamental investigations are necessary to explore the contributions of both the internal and external distribution of the catalytic active sites present for the bulk M1 phase for ODHE.

2.7. Effects of promoters

Early research indicated catalyst reducibility is a key factor in enhancing the performance of the ODHE reaction by the bulk M1 phase catalyst [165] which led to the addition of several oxide promoters for MoVNbTe mixed oxide catalysts that would increase their reducibility. Doping Bi into the M1 phase by spray-dry method resulted in a change in morphology (as shown by TEM) [180,181]. These Bi-doped M1 phase particles exhibited distorted growth patterns, non-preferential orientation, and a reduction in size when compared to undoped M1 phase particles [180,181]. Furthermore, despite the lower M1/M2 ratio, the Bi-doped M1 catalysts demonstrated better ethane conversion and similar ethylene selectivity compared to the undoped versions [180, 181]. This might be partially explained by the higher surface Te^{4+} retention [180] and higher surface V^{5+} (to a small extent Mo^{6+}) in Bi-doped samples [181], as demonstrated by UHV XPS. Meanwhile, the K-doped M1 phase catalyst, with a higher M2/M1 ratio, exhibited significantly lower ethane conversion, which was loosely attributed to lower surface V^{5+} (UHV XPS) compared to the undoped M1 phase catalyst [181]. The introduction of MnO_x nanoparticles lowered ethane conversion and selectivity to ethylene for ODHE reaction [75]. Xin *et al.* employed MnO_x-free and MnO_x HT M1 catalysts with the same bulk (ICP) and surface (UHV XPS) M/V/Nb/Te compositions [75]. The reduction in ethane conversion and ethylene selectivity occurred for the MnO_x M1 catalyst despite its higher surface V^{5+} cation content compared to the MnO_x-free counterpart (66 % > 56 % of total surface V) [75]. The SiO_x-promoted SL M1 phase exhibited higher ethane conversion and similar ethylene selectivity as the SiO_x-free M1 phase [90], probably due to the higher surface area of the Si-promoted M1 catalyst (23.8 m^2/g) versus that of the unpromoted M1 catalyst (4.6 m^2/g) [90]. Impregnation of the CeO_x promoter during [147] or after [78,166] the HT M1 synthesis step resulted in a partially amorphous surface, as indicated by SEM and TEM measurements [78,147,166]. These CeO_x-promoted M1 catalysts exhibited higher ethane conversion and similar [147] or lower [78,166] ethylene selectivity than the CeO_x-free M1 catalyst. The corresponding UHV XPS measurements demonstrated an increase in the concentration of V^{5+} in the surface region of MoVNbTe catalysts [78,166] from the addition of CeO_x promoter. Post-synthesis via physical mixing and sol-gel method to obtain the TiO_x-promoted M1 phase was conducted by Dang *et al.* [77,79]. The surface areas of these 40 wt% TiO_x-promoted M1 phase catalysts are 3–4 times larger than the unpromoted M1 phase catalysts [77,79]. Therefore, the observed enhanced catalytic activities of these TiO_x-promoted M1 phase catalysts can arise from the increase in surface area. Adding Nd, Mn, Ga, and Ge via spray-drying produced positive catalytic effects for ODHE by the M1 phase [182]. The amount of surface V^{5+} and Mo^{6+} (UHV XPS) was found to vary independently of additives [182]. In general, the addition of promoters enhances the surface V^{5+} content and is typically associated with the increase in observed activity. However, it is difficult to assign this increased V^{5+} concentration to the catalytic enhancement of ODHE without a fundamental understanding of the active sites and

Table 2
Literature proposals of the functions of V, Mo, Nb, Te oxide sites for ODHE for the bulk M1 phase catalyst from the different reported studies.

Element	Proposal	Reference
Mo	N/A	
V	V^{5+} sites abstract a methyl-H from ethane	[86]
	Near-surface region V^{5+} cations act as the surface active sites, performing the first H-abstraction step	[74,98]
Nb	Nb addition enhances the surface area of the catalyst and prevents MoO_2 (Mo^{4+}) formation	[157]
Te	Te prevents the formation of non-selective Mo-containing crystalline phases	[52,68,69, 105]
	Te cations stabilize the bulk crystalline M1 phase catalyst	[98]

the ODHE reaction mechanism by the bulk MoVNbTe mixed oxide catalysts.

3. Conclusions

The literature review discussed above indicates that much is still unknown about the fundamentals of the ODHE reaction by the bulk crystalline MoVNbTe mixed oxide M1 phase catalyst.

(i) The synthesis of the bulk MoVNbTe mixed oxide catalysts typically employs the SL and HT methods. The HT preparation is preferred to the SL preparation since it results in a catalyst with a higher BET surface area and higher crystalline M1/M2 ratio, both of which are desirable. Other pre-calcination treatments for HT including spray-dry and sol-gel require more investigations into their benefits.
(ii) The bulk M1, M2, and other secondary bulk phases co-exist in the synthesized catalyst, which necessitates post-treatments using hydrogen peroxide, oxalic acid, or nitric acid to selectively remove the undesired components (bulk M2 and other secondary bulk metal oxide phases).
(iii) A residual amorphous overlayer phase on the crystalline bulk M1 phase also appears to be present after the post-treatment. This could be the location of the active surface sites on the M1 phase catalyst, which requires surface-sensitive tools to examine.
(iv) The crystalline bulk M1 phase appears to be stable under the typical ODHE reaction conditions. The ability of Te to maintain the highest oxidation state + 4 is critical for the stability of the bulk M1 phase.
(v) The surface of the crystalline bulk M1 phase is dynamic and varies with the reaction environment.
(vi) The VO_x sites in the surface region appear to undergo redox, suggesting that they are the catalytic active sites involved in the activation of ethane.
(vii) The MoO_x sites in the surface region probably also undergo redox, but are sluggish in comparison to the VO_x sites.
(viii) The NbO_x and TeO_x sites appear to stabilize the crystalline bulk M1 structure under reaction conditions.
(ix) The ODHE reaction is strongly dependent on the ethane partial pressure (reaction orders of ~1.3–1.8), suggesting that the breaking of the C-H bond of ethane is RDS.
(x) The ODHE reaction is weakly dependent on the molecular O_2 partial pressure (reaction orders of ~0.1–0.3), suggesting that lattice oxygen atoms participate via the Mars-van Krevelen mechanism.
(xi) Due to the complexity of the bulk M1 phase, involvement of DFT is required to untangle complex vibrational assignments using vibrational spectroscopy techniques (i.e., Raman, FTIR).
(xii) The lack of modern *in situ* and *operando* surface characterization studies of the crystalline bulk M1 phase catalyst under ODHE reaction conditions has prevented identifying the catalytic active sites (external surface sites, internal surface sites in the pores and the amorphous overlayer) and their roles during the ODHE reaction. The complex ODHE reaction mechanism on the bulk MoVNbTe mixed oxide catalyst can be established once the identification of the active sites is verified.
(xiii) A fundamental structure-activity/selectivity model for the ODHE reaction based on supporting data will also require the application of modern *in situ* and *operando* surface characterization coupled with DFT studies.
(xiv) For several safety and environmental concerns, ODHE with soft oxidants (CO_2) has become popular, and further investigations are required for studies with the bulk M1 phase catalyst.
(xv) More efficient catalysts require a fundamental understanding of catalytic active sites and the ODHE reaction mechanism. Promoting the M1 phase with metal and metal oxides can improve catalytic activity and allow a longer catalyst lifetime.

CRediT authorship contribution statement

Dang D. Nguyen: Investigation, Writing - Original Draft, Writing- Reviewing and Editing, Visualization.; **Bar Mosevitzky Lis:** Investigation, Writing - Original Draft, Writing- Reviewing and Editing.; **Israel E. Wachs:** Conceptualization, Supervision, Writing- Reviewing and Editing, Project administration, Funding acquisition.

Declaration of Competing Interest

The authors declare that they have no known competing financial interests or personal relationships that could have appeared to influence the work reported in this paper.

Acknowledgments

This work was supported by the U.S. National Science Foundation (NSF) under award # CBET-2221714.

Data availability

Data will be made available on request.

References

[1] S. Najari, S. Saeidi, P. Concepcion, D.D. Dionysiou, S.K. Bhargava, A.F. Lee, K. Wilson, Oxidative dehydrogenation of ethane: catalytic and mechanistic aspects and future trends, Chem. Soc. Rev. 50 (2021) 4564–4605, https://doi.org/10.1039/D0CS01518K.
[2] Ethylene Production, Emerson (2010). ⟨https://www.emerson.com/documents/automation/manuals-guides-chemical-sourcebook-chapter-1-2-ethylene-production-polysilicone-production-fisher-en-138242.pdf⟩.
[3] Ethylene, American Chemical Society (2013). ⟨https://www.acs.org/molecule-of-the-week/archive/e/ethylene.html⟩.
[4] Production capacity of ethylene worldwide from 2018 to 2021, Statista (2023). ⟨https://www.statista.com/statistics/1067372/global-ethylene-production-capacity/⟩#:~:text=The production capacity of ubiquitous,percent in comparison with 2018.
[5] Market size of ethylene worldwide in 2021, with a forecast until 2030, Statista (2023). ⟨https://www.statista.com/statistics/1349781/ethylene-global-market-size⟩/#:~:text=In 2021%2C the global market,used in the plastic industry.
[6] Ethylene demand and production capacity worldwide from 2015 to 2022, Statista (2023). ⟨https://www.statista.com/statistics/1246694/ethylene-demand-capacity-forecast-worldwide⟩/#:~:text=Global ethylene demand and capacity 2015-2022&text=Ethylene demand was forecast to,rise to 196 million tons.
[7] Global Ethylene Market (by Production Capacity & Demand): Insights & Forecast with Potential Impact of COVID-19 (2023-2027), Research and Markets (2023). ⟨https://www.researchandmarkets.com/reports/5531033/global-ethylene-market-by-production-capacity-and⟩.
[8] Ethylene Global Market Report 2023, Research and Markets (2023). ⟨https://www.researchandmarkets.com/reports/5733833/ethylene-global-market-report⟩.
[9] Decode the Future of Ethylene, Chemanalyst (2023). ⟨https://www.chemanalyst.com/industry-report/ethylene-market-638⟩.
[10] E. Worrell, D. Phylipsen, D. Einstein, N. Martin, Energy Use and Energy Intensity of the U.S. Chemical Industry, Berkeley, CA, 2000.
[11] Y. Gao, L. Neal, D. Ding, W. Wu, C. Baroi, A.M. Gaffney, F. Li, Recent Advances in Intensified Ethylene Production—A Review, ACS Catal. 9 (2019) 8592–8621, https://doi.org/10.1021/acscatal.9b02922.
[12] J. Cantrell, J.A. Bullin, G. McIntyre, C.R. Butts, B. Cheatham, Consider GTL as an economic alternative for stranded natural gas and ethane, Hydrocarb. Process. 92 (2013) 77–80. ⟨https://link.gale.com/apps/doc/A347660006/AONE?u=anon~5b2d30b4&sid=googleScholar&xid=2ef28fc9⟩.
[13] C.A. Gärtner, A.C. van Veen, J.A. Lercher, Oxidative Dehydrogenation of Ethane: Common Principles and Mechanistic Aspects, ChemCatChem 5 (2013) 3196–3217, https://doi.org/10.1002/cctc.201200966.
[14] I. Amghizar, L.A. Vandewalle, K.M. Van Geem, G.B. Marin, New Trends in Olefin Production, Engineering 3 (2017) 171–178, https://doi.org/10.1016/J.ENG.2017.02.006.
[15] T. Baidya, N. van Vegten, A. Baiker, Selective Conversion of Ethane to Ethene via Oxidative Dehydrogenation Over Ca-doped ThO2 Using CO2 as Oxidant, Top. Catal. 54 (2011) 881–887, https://doi.org/10.1007/s11244-011-9696-8.

[16] V.N. Cavaliere, M.G. Crestani, B. Pinter, M. Pink, C.-H. Chen, M.-H. Baik, D. J. Mindiola, Room Temperature Dehydrogenation of Ethane to Ethylene, J. Am. Chem. Soc. 133 (2011) 10700–10703, https://doi.org/10.1021/ja202316m.

[17] I. Sinev, T. Kardash, N. Kramareva, M. Sinev, O. Tkachenko, A. Kucherov, L. M. Kustov, Interaction of vanadium containing catalysts with microwaves and their activation in oxidative dehydrogenation of ethane, Catal. Today 141 (2009) 300–305, https://doi.org/10.1016/j.cattod.2008.04.021.

[18] T. Ren, M. Patel, K. Blok, Olefins from conventional and heavy feedstocks: Energy use in steam cracking and alternative processes, Energy 31 (2006) 425–451, https://doi.org/10.1016/j.energy.2005.04.001.

[19] A. Corma, E. Corresa, Y. Mathieu, L. Sauvanaud, S. Al-Bogami, M.S. Al-Ghrami, A. Bourane, Crude oil to chemicals: light olefins from crude oil, Catal. Sci. Technol. 7 (2017) 12–46, https://doi.org/10.1039/C6CY01886F.

[20] V.P. Haribal, L.M. Neal, F. Li, Oxidative dehydrogenation of ethane under a cyclic redox scheme – Process simulations and analysis, Energy 119 (2017) 1024–1035, https://doi.org/10.1016/j.energy.2016.11.039.

[21] P. Sun, G. Siddiqi, W.C. Vining, M. Chi, A.T. Bell, Novel Pt/Mg(In)(Al)O catalysts for ethane and propane dehydrogenation, J. Catal. 282 (2011) 165–174, https://doi.org/10.1016/j.jcat.2011.06.008.

[22] M.M. Forde, R.D. Armstrong, C. Hammond, Q. He, R.L. Jenkins, S.A. Kondrat, N. Dimitratos, J.A. Lopez-Sanchez, S.H. Taylor, D. Willock, C.J. Kiely, G. J. Hutchings, Partial Oxidation of Ethane to Oxygenates Using Fe- and Cu-Containing ZSM-5, J. Am. Chem. Soc. 135 (2013) 11087–11099, https://doi.org/10.1021/ja403060n.

[23] I.A. Bakare, S.A. Mohamed, S. Al-Ghamdi, S.A. Razzak, M.M. Hossain, H.I. de Lasa, Fluidized bed ODH of ethane to ethylene over VOx–MoOx/γ-Al2O3 catalyst: Desorption kinetics and catalytic activity, Chem. Eng. J. 278 (2015) 207–216, https://doi.org/10.1016/j.cej.2014.09.114.

[24] S. MacIntyre, W.U.S. Wilczewski, Ethane Consumption, Exports to Increase as New Petrochemical Plants Come Online, U. S. Energy Inf. Adm.: Wash., D. C. (2018), 1., (n.d.).

[25] S. MacIntyre, Ethane Production Growth Led to Record U.S. Natural Gas Plant Liquids Production in 2017. U.S. Energy Information Administration: Washington, D. C. (2018) p 2., (n.d.).

[26] W. Wilczewski, The United States Expands Its Role as World's Leading Ethane Exporter. U.S. Energy Information Administration: Washington, D. C. (2019) p 2., (n.d.).

[27] Annual Energy Outlook, U.S. Energy Information Administration (2021). ⟨https://www.eia.gov/outlooks/aeo/tables_side.php⟩.

[28] Lewandowski, S. Ethylene - Global. 4th Annual Asia Chemical Conference 2016: Singapore 2016, p 31., (n.d.).

[29] Global Ethylene Industry Outlook to 2023 – Capacity and Capital Expenditure Forecasts with Details of All Active and Planned Plants, London, 2019.

[30] M.V. Martínez-Huerta, X. Gao, H. Tian, I. Wachs, J.L.G. Fierro, M.A. Bañares, Oxidative dehydrogenation of ethane to ethylene over alumina-supported vanadium oxide catalysts: Relationship between molecular structures and chemical reactivity, Catal. Today 118 (2006) 279–287, https://doi.org/10.1016/j.cattod.2006.07.034.

[31] H.H. Kung, Oxidative Dehydrogenation of Light (C2 to C4) Alkanes, Adv. Catal. 40 (1994) 1–38, https://doi.org/10.1016/S0360-0564(08)60655-0.

[32] M.M. Bhasin, Is True Ethane Oxydehydrogenation Feasible? Top. Catal. 23 (2003) 145–149, https://doi.org/10.1023/A:1024884623238.

[33] H.R. Shahhosseini, S. Saeidi, S. Najari, F. Gallucci, Comparison of conventional and spherical reactor for the industrial auto-thermal reforming of methane to maximize synthesis gas and minimize CO2, Int. J. Hydrog. Energy 42 (2017) 19798–19809, https://doi.org/10.1016/j.ijhydene.2017.06.192.

[34] D. Iranshahi, N. Hamedi, M. Nategh, R. Saeedi, S. Saeidi, Thermal Integration of Sulfuric Acid and Continuous Catalyst Regeneration of Naphtha Reforming Plants, Chem. Eng. Technol. 41 (2018) 637–655, https://doi.org/10.1002/ceat.201600733.

[35] D. Iranshahi, P. Salimi, Z. Pourmand, S. Saeidi, J.J. Klemeš, Utilising a radial flow, spherical packed-bed reactor for auto thermal steam reforming of methane to achieve a high capacity of H2 production, Chem. Eng. Process. 120 (2017) 258–267, https://doi.org/10.1016/j.cep.2017.07.020.

[36] O.O. James, S. Mandal, N. Alele, B. Chowdhury, S. Maity, Lower alkanes dehydrogenation: Strategies and reaction routes to corresponding alkenes, Fuel Process. Technol. 149 (2016) 239–255, https://doi.org/10.1016/j.fuproc.2016.04.016.

[37] B. Solsona, P. Concepción, S. Hernández, B. Demicol, J.M.L. Nieto, Oxidative dehydrogenation of ethane over NiO–CeO2 mixed oxides catalysts, Catal. Today 180 (2012) 51–58, https://doi.org/10.1016/j.cattod.2011.03.056.

[38] B. Solsona, J.M. López Nieto, P. Concepción, A. Dejoz, F. Ivars, M.I. Vázquez, Oxidative dehydrogenation of ethane over Ni–W–O mixed metal oxide catalysts, J. Catal. 280 (2011) 28–39, https://doi.org/10.1016/j.jcat.2011.02.010.

[39] J.M.L. Nieto, The selective oxidative activation of light alkanes. From supported vanadia to multicomponent bulk V-containing catalysts, Top. Catal. 41 (2006) 3–15, https://doi.org/10.1007/s11244-006-0088-4.

[40] Transforming Our World: The 2030 Agenda for Sustainable Development, A/RES/70/1. UN General Assembly 2015, p 35., n.d.

[41] F. Cavani, N. Ballarini, A. Cericola, Oxidative dehydrogenation of ethane and propane: How far from commercial implementation? Catal. Today 127 (2007) 113–131, https://doi.org/10.1016/j.cattod.2007.05.009.

[42] J.-P. Lange, R.J. Schoonebeek, P.D.L. Mercera, F.W. van Breukelen, Oxycracking of hydrocarbons: chemistry, technology and economic potential, Appl. Catal. A Gen. 283 (2005) 243–253, https://doi.org/10.1016/j.apcata.2005.01.011.

[43] E.M. Thorsteinson, T.P. Wilson, F.G. Young, P.H. Kasai, The oxidative dehydrogenation of ethane over catalysts containing mixed oxides of molybdenum and vanadium, J. Catal. 52 (1978) 116–132, https://doi.org/10.1016/0021-9517(78)90128-8.

[44] J.A. Lercher, F.N. Naraschewski, C–H Activation of Alkanes in Selective Oxidation Reactions on Solid Oxide Catalysts, in: Nanostructured Catalysts: Selective Oxidations, Royal Society of Chemistry, Cambridge, 2011, pp. 5–32.

[45] M.D. Argyle, K. Chen, A.T. Bell, E. Iglesia, Ethane Oxidative Dehydrogenation Pathways on Vanadium Oxide Catalysts, J. Phys. Chem. B 106 (2002) 5421–5427, https://doi.org/10.1021/jp0144552.

[46] M.C. Abello, M.F. Gomez, O. Ferretti, Mo/γ-Al2O3 catalysts for the oxidative dehydrogenation of propane. Appl. Catal. A Gen. 207 (2001) 421–431, https://doi.org/10.1016/S0926-860X(00)00680-3.

[47] C. Liu, U.S. Ozkan, Effect of chlorine on redox and adsorption characteristics of Mo/Si:Ti catalysts in the oxidative dehydrogenation of ethane, J. Mol. Catal. A Chem. 220 (2004) 53–65, https://doi.org/10.1016/j.molcata.2004.03.049.

[48] C. Liu, U.S. Ozkan, Spectroscopic and Structural Characterization of Chlorine Loading Effects on Mo/Si:Ti Catalysts in Oxidative Dehydrogenation of Ethane, J. Phys. Chem. A 109 (2005) 1260–1268, https://doi.org/10.1021/jp045726m.

[49] K. Karim, A. Mamedov, M.H. Al-Hazmi, N. Al-Andis, Oxidative dehydrogenation of ethane over MoVMnW oxide catalysts, React. Kinet. Catal. Lett. 80 (2003) 3–11, https://doi.org/10.1023/A:1026012203802.

[50] A.S.H. Kumar, K. Upendar, A. Qiao, P.S.N. Rao, N. Lingaiah, V.N. Kalevaru, A. Martin, Ch Sailu, P.S.S. Prasad, Selective oxidative dehydrogenation of ethane over MoO3/V2O5–Al2O3 catalysts: Heteropolymolybdate as a precursor for MoO3, Catal. Commun. 33 (2013) 76–79, https://doi.org/10.1016/j.catcom.2012.12.012.

[51] F. Rahman, K.F. Loughlin, M.A. Al-Saleh, M.R. Saeed, N.M. Tukur, M.M. Hossain, K. Karim, A. Mamedov, Kinetics and mechanism of partial oxidation of ethane to ethylene and acetic acid over MoV type catalysts, Appl. Catal. A Gen. 375 (2010) 17–25, https://doi.org/10.1016/j.apcata.2009.11.026.

[52] J.M. López Nieto, P. Botella, P. Concepción, A. Dejoz, M.I. Vázquez, Oxidative dehydrogenation of ethane on Te-containing MoVNbO catalysts, Catal. Today 91–92 (2004) 241–245, https://doi.org/10.1016/j.cattod.2004.03.040.

[53] J.M.L. Nieto, P. Botella, M.I. Vázquez, A. Dejoz, The selective oxidative dehydrogenation of ethane over hydrothermally synthesised MoVTeNb catalysts, Chem. Commun. (2002) 1906–1907, https://doi.org/10.1039/B204037A.

[54] E. Heracleous, A.T. Lee, K.S. Wilson, A.A. Lemonidou, Investigation of Ni-based alumina-supported catalysts for the oxidative dehydrogenation of ethane to ethylene: structural characterization and reactivity studies, J. Catal. 231 (2005) 159–171, https://doi.org/10.1016/j.jcat.2005.01.015.

[55] S. Wang, K. Murata, T. Hayakawa, S. Hamakawa, K. Suzuki, Selective oxidation of ethane and propane over sulfated zirconia-supported nickel oxide catalysts, J. Chem. Technol. Biotechnol. 76 (2001) 265–272, https://doi.org/10.1002/jctb.373.

[56] Y. Brik, M. Kacimi, M. Ziyad, F. Bozon-Verduraz, Titania-Supported Cobalt and Cobalt–Phosphorus Catalysts: Characterization and Performances in Ethane Oxidative Dehydrogenation, J. Catal. 202 (2001) 118–128, https://doi.org/10.1006/jcat.2001.3262.

[57] H.M. Swaan, Y. Li, K. Seshan, J.G. Van Ommen, J.R.H. Ross, The oxidative coupling of methane and the oxidative dehydrogenation of ethane over a niobium promoted lithium doped magnesium oxide catalyst, Catal. Today 16 (1993) 537–546, https://doi.org/10.1016/0920-5861(93)80094-H.

[58] S. Gaab, M. Machli, R.K. Grasselli, J.A. Lercher, Oxidative Dehydrogenation of Ethane Over Novel Li/Dy/Mg Mixed Oxides: Structure–Activity Study, Top. Catal. 23 (2003) 151–158, https://doi.org/10.1023/a:1024836707308.

[59] D.J. Wang, M.P. Rosynek, J.H. Lunsford, The Effect of Chloride Ions on a Li+ -MgO Catalyst for the Oxidative Dehydrogenation of Ethane, J. Catal. 151 (1995) 155–167, https://doi.org/10.1006/jcat.1995.1018.

[60] E.M. Kennedy, N.W. Cant, Comparison of the oxidative dehydrogenation of ethane and oxidative coupling of methane over rare earth oxides, Appl. Catal. 75 (1991) 321–330, https://doi.org/10.1016/S0166-9834(00)83141-3.

[61] L. Ji, J. Liu, X. Chen, M. Li, The oxidative dehydrogenation of ethane over alkali-doped lanthanum-calcium oxide catalysts, Catal. Lett. 39 (1996) 247–252, https://doi.org/10.1007/BF00805590.

[62] V.R. Choudhary, S.A.R. Mulla, V.H. Rane, Coupling of exothermic and endothermic reactions in oxidative conversion of ethane to ethylene over alkaline earth promoted La2O3 catalysts in presence of limited O2, Appl. Energy 66 (2000) 51–62, https://doi.org/10.1016/S0306-2619(99)00040-9.

[63] X. Lin, C.A. Hoel, W.M.H. Sachtler, K.R. Poeppelmeier, E. Weitz, Oxidative dehydrogenation (ODH) of ethane with O2 as oxidant on selected transition metal-loaded zeolites, J. Catal. 265 (2009) 54–62, https://doi.org/10.1016/j.jcat.2009.04.007.

[64] G. Busca, E. Finocchio, V. Lorenzelli, G. Ramis, M. Baldi, IR studies on the activation of C–H hydrocarbon bonds on oxidation catalysts, Catal. Today 49 (1999) 453–465, https://doi.org/10.1016/S0920-5861(98)00441-6.

[65] M.C. Huff, I.P. Androulakis, J.H. Sinfelt, S.C. Reyes, The Contribution of Gas-Phase Reactions in the Pt-Catalyzed Conversion of Ethane–Oxygen Mixtures, J. Catal. 191 (2000) 46–54, https://doi.org/10.1006/jcat.1999.2798.

[66] A.M. Gaffney, O.M. Mason, Ethylene production via Oxidative Dehydrogenation of Ethane using M1 catalyst, Catal. Today 285 (2017) 159–165, https://doi.org/10.1016/j.cattod.2017.01.020.

[67] Z. Han, X. YI, Q. XIE, R. Li, H. Lin, Y. He, L. Chen, W. Weng, H. Wan, Oxidative dehydrogenation of ethane over MoVTeNbO catalyst prepared by a slurry method, Chinese, J. Catal. 26 (2005) 441–442.

[68] P. Botella, E. García-González, A. Dejoz, J.M.L. Nieto, M.I. Vázquez, J. González-Calbet, Selective oxidative dehydrogenation of ethane on MoVTeNbO mixed metal oxide catalysts, J. Catal. 225 (2004) 428–438, https://doi.org/10.1016/j.jcat.2004.04.024.
[69] B. Solsona, M. Vázquez, F. Ivars, A. Dejoz, P. Concepción, J. Nieto, Selective oxidation of propane and ethane on diluted Mo–V–Nb–Te mixed-oxide catalysts, J. Catal. 252 (2007) 271–280, https://doi.org/10.1016/j.jcat.2007.09.019.
[70] S.C. Arnold, A.M. Gaffney, R. Song, C.Y. Yeh, Process for producing ethylene via oxidative dehydrogenation (ODH) of ethane, WO2010115108 A1, 2010.
[71] J.S. Valente, H. Armendáriz-Herrera, R. Quintana-Solórzano, P. del Ángel, N. Nava, A. Massó, J.M.L.ópez Nieto, Chemical, Structural, and Morphological Changes of a MoVTeNb Catalyst during Oxidative Dehydrogenation of Ethane, ACS Catal. 4 (2014) 1292–1301, https://doi.org/10.1021/cs500143j.
[72] D. Hartmann, A. Meiswinkel, C. Thaller, M. Bock, L. Alvarado, M.C. Sanchez-Sanchez, A.C. van Veen, J.A. Lercher, Mo-V-Te-Nb oxides as catalysts for ethene production by oxidative dehydrogenation of ethane, Hamburg (2013).
[73] T.T. Nguyen, B. Deniau, P. Delichere, J.-M.M. Millet, Influence of the Content and Distribution of Vanadium in the M1 Phase of the MoVTe(Sb)NbO Catalysts on their Catalytic Properties in Light Alkanes Oxidation, Top. Catal. 57 (2014) 1152–1162, https://doi.org/10.1007/s11244-014-0282-8.
[74] B. Chu, L. Truter, T.A. Nijhuis, Y. Cheng, Performance of phase-pure M1 MoVNbTeOx catalysts by hydrothermal synthesis with different post-treatments for the oxidative dehydrogenation of ethane, Appl. Catal. A Gen. 498 (2015) 99–106, https://doi.org/10.1016/j.apcata.2015.03.039.
[75] X. Chen, D. Dang, H. An, B. Chu, Y. Cheng, MnOx promoted phase-pure M1 MoVNbTe oxide for ethane oxidative dehydrogenation, J. Taiwan Inst. Chem. Eng. 95 (2019) 103–111, https://doi.org/10.1016/j.jtice.2018.10.004.
[76] L. Annamalai, S. Ezenwa, Y. Dang, H. Tan, S.L. Suib, P. Deshlahra, Comparison of structural and catalytic properties of monometallic Mo and V oxides and M1 phase mixed oxides for oxidative dehydrogenation, Catal. Today 368 (2021) 28–45, https://doi.org/10.1016/j.cattod.2020.04.046.
[77] Y. Chen, D. Dang, B. Yan, Y. Cheng, Mixed Metal Oxides of M1 MoVNbTeOx and TiO2 as Composite Catalyst for Oxidative Dehydrogenation of Ethane, Catalysts 12 (2022) 71, https://doi.org/10.3390/catal12010071.
[78] B. Chu, H. An, T.A. Nijhuis, J.C. Schouten, Y. Cheng, A self-redox pure-phase M1 MoVNbTeOx/CeO2 nanocomposite as a highly active catalyst for oxidative dehydrogenation of ethane, J. Catal. 329 (2015) 471–478, https://doi.org/10.1016/j.jcat.2015.06.009.
[79] D. Dang, Y. Chen, X. Chen, K. Feng, B. Yan, Y. Cheng, Phase-pure M1 MoVNbTeOx/TiO2 nanocomposite catalysts: high catalytic performance for oxidative dehydrogenation of ethane, Catal. Sci. Technol. 12 (2022) 1211–1219, https://doi.org/10.1039/D1CY01749G.
[80] Y. Chen, B. Yan, Y. Cheng, Microporous exposure on catalytic performance of MoVNbTeOx mixed metal oxides in the oxidative dehydrogenation of ethane, J. Catal. 426 (2023) 308–318, https://doi.org/10.1016/j.jcat.2023.07.025.
[81] A. de Arriba, G. Sánchez, R. Sánchez-Tovar, P. Concepción, R. Fernández-Domene, B. Solsona, J.M.L.ópez Nieto, On the selectivity to ethylene during ethane ODH over M1-based catalysts. A surface and electrochemical study, Catal. Today 418 (2023) 114122, https://doi.org/10.1016/j.cattod.2023.114122.
[82] S. Lwin, W. Diao, C. Baroi, A. Gaffney, R. Fushimi, Characterization of MoVTeNbOx Catalysts during Oxidation Reactions Using In Situ/Operando Techniques: A Review, Catalysts 7 (2017) 109, https://doi.org/10.3390/catal7040109.
[83] M.A. Bañares, Supported metal oxide and other catalysts for ethane conversion: a review, Catal. Today 51 (1999) 319–348, https://doi.org/10.1016/S0920-5861(99)00053-X.
[84] T. Ushikubo, K. Oshima, A. Kayou, M. Hatano, Ammoxidation of propane over Mo-V-Nb-Te mixed oxide catalysts, in: 1997: pp. 473–480. https://doi.org/10.1016/S0167-2991(97)80871-3.
[85] J.C. Védrine, Heterogeneous Partial (amm)Oxidation and Oxidative Dehydrogenation Catalysis on Mixed Metal Oxides, Catalysts 6 (2016) 22, https://doi.org/10.3390/catal6020022.
[86] Q. Xie, L. Chen, W. Weng, H. Wan, Preparation of MoVTe(Sb)Nb mixed oxide catalysts using a slurry method for selective oxidative dehydrogenation of ethane, J. Mol. Catal. A Chem. (2005), https://doi.org/10.1016/j.molcata.2005.07.004.
[87] I.E. Wachs, J.-M. Jehng, W. Ueda, Determination of the Chemical Nature of Active Surface Sites Present on Bulk Mixed Metal Oxide Catalysts, J. Phys. Chem. B 109 (2005) 2275–2284, https://doi.org/10.1021/jp048839e.
[88] B. Deniau, G. Bergeret, B. Jouguet, J.L. Dubois, J.M.M. Millet, Preparation of Single M1 Phase MoVTe(Sb)NbO Catalyst: Study of the Effect of M2 Phase Dissolution on the Structure and Catalytic Properties, Top. Catal. 50 (2008) 33–42, https://doi.org/10.1007/s11244-008-9104-1.
[89] F.N. Naraschewski, C. Praveen Kumar, A. Jentys, J.A. Lercher, Phase formation and selective oxidation of propane over MoVTeNbOx catalysts with varying compositions, Appl. Catal. A Gen. 391 (2011) 63–69, https://doi.org/10.1016/j.apcata.2010.07.005.
[90] T.T. Nguyen, M. Aouine, J.M.M. Millet, Optimizing the efficiency of MoVTeNbO catalysts for ethane oxidative dehydrogenation to ethylene, Catal. Commun. 21 (2012) 22–26, https://doi.org/10.1016/j.catcom.2012.01.026.
[91] M. Hävecker, S. Wrabetz, J. Kröhnert, L.-I. Csepei, R. Naumann d'Alnoncourt, Y. V. Kolen'ko, F. Girgsdies, R. Schlögl, A. Trunschke, Surface chemistry of phase-pure M1 MoVTeNb oxide during operation in selective oxidation of propane to acrylic acid, J. Catal. 285 (2012) 48–60, https://doi.org/10.1016/j.jcat.2011.09.012.
[92] P. Botella, B. Solsona, A. Martinez-Arias, J.M. López Nieto, Selective Oxidation of Propane to Acrylic Acid on MoVNbTe Mixed Oxides Catalysts Prepared by Hydrothermal, Synth., Catal. Lett. 74 (2001), https://doi.org/10.1023/A:1016614132694.
[93] D.A. Svintsitskiy, T.Y. Kardash, E.V. Lazareva, V.M. Bondareva, X-ray-induced transformations on the surface of MoVNbTe mixed oxide catalyst: An XPS study, Appl. Surf. Sci. 535 (2021) 147676, https://doi.org/10.1016/j.apsusc.2020.147676.
[94] J.M.M. Millet, H. Roussel, A. Pigamo, J.L. Dubois, J.C. Jumas, Characterization of tellurium in MoVTeNbO catalysts for propane oxidation or ammoxidation, Appl. Catal. A Gen. 232 (2002) 77–92, https://doi.org/10.1016/S0926-860X(02)00078-9.
[95] P. Beato, A. Blume, F. Girgsdies, R.E. Jentoft, R. Schlögl, O. Timpe, A. Trunschke, G. Weinberg, Q. Basher, F.A. Hamid, S.B.A. Hamid, E. Omar, L. Mohd Salim, Analysis of structural transformations during the synthesis of a MoVTeNb mixed oxide catalyst, Appl. Catal. A Gen. 307 (2006) 137–147, https://doi.org/10.1016/j.apcata.2006.03.014.
[96] P. DeSanto, D.J. Buttrey, R.K. Grasselli, C.G. Lugmair, A.F. Volpe, B.H. Toby, T. Vogt, Structural Characterization of the Orthorhombic Phase M1 in MoVNbTeO Propane Ammoxidation Catalyst, Top. Catal. 23 (2003) 23–38, https://doi.org/10.1023/A:1024812101856.
[97] H. Watanabe, Y. Koyasu, New synthesis route for Mo–V–Nb–Te mixed oxides catalyst for propane ammoxidation, Appl. Catal. A Gen. 194–195 (2000) 479–485, https://doi.org/10.1016/S0926-860X(99)00394-4.
[98] X. Chen, Q. Yang, B. Chu, H. An, Y. Cheng, Valence variation of phase-pure M1 MoVNbTe oxide by plasma treatment for improved catalytic performance in oxidative dehydrogenation of ethane, RSC Adv. 5 (2015) 91295–91301, https://doi.org/10.1039/C5RA16517B.
[99] B. Chu, H. An, X. Chen, Y. Cheng, Phase-pure M1 MoVNbTeOx catalysts with tunable particle size for oxidative dehydrogenation of ethane, Appl. Catal. A Gen. 524 (2016) 56–65, https://doi.org/10.1016/j.apcata.2016.05.026.
[100] A. Tompos, M. Sanchez-Sanchez, L. Végvári, G.P. Szijjártó, J.L. Margitfalvi, A. Trunschke, R. Schlögl, K. Wanninger, G. Mestl, Combinatorial optimization and synthesis of multiple promoted MoVNbTe catalysts for oxidation of propane to acrylic acid, Catal. Today 363 (2021) 45–54, https://doi.org/10.1016/j.cattod.2019.03.047.
[101] Y. Wang, Y. Fan, S. Li, Y. Wang, Y. Chen, D. Liu, W. Wei, S. Yu, Crystal structure and catalytic performance for direst oxidation of propylene to acrylic acid of MoVTeNbOx prepared by high-pressure hydrothermal synthesis, Resour. Chem. Mater. 1 (2022) 211–221, https://doi.org/10.1016/j.recm.2022.07.004.
[102] A. Celaya Sanfiz, T.W. Hansen, F. Girgsdies, O. Timpe, E. Rödel, T. Ressler, A. Trunschke, R. Schlögl, Preparation of Phase-Pure M1 MoVTeNb Oxide Catalysts by Hydrothermal Synthesis—Influence of Reaction Parameters on Structure and Morphology, Top. Catal. 50 (2008) 19–32, https://doi.org/10.1007/s11244-008-9106-z.
[103] M. Baca, A. Pigamo, J.L. Dubois, J.M.M. Millet, Propane Oxidation on MoVTeNbO Mixed Oxide Catalysts: Study of the Phase Composition of Active and Selective Catalysts, Top. Catal. 23 (2003) 39–46, https://doi.org/10.1023/A:1024864118695.
[104] K. Oshihara, Y. Nakamura, M. Sakuma, W. Ueda, Hydrothermal synthesis of novel crystalline Mo–V–M–O (M = Al, Ga, Fe) mixed oxide in the presence of triethylammonium chloride and their catalytic performance for selective ethane oxidation, Catal. Today 71 (2001) 153–159, https://doi.org/10.1016/S0920-5861(01)00451-5.
[105] P. Botella, A. Dejoz, M.C. Abello, M.I. Vázquez, L. Arrúa, J.M.L.ópez Nieto, Selective oxidation of ethane: Developing an orthorhombic phase in Mo–V–X (X=Nb, Sb, Te) mixed oxides, Catal. Today 142 (2009) 272–277, https://doi.org/10.1016/j.cattod.2008.09.016.
[106] D. Melzer, G. Mestl, K. Wanninger, Y. Zhu, N.D. Browning, M. Sanchez-Sanchez, J.A. Lercher, Design and synthesis of highly active MoVTeNb-oxides for ethane oxidative dehydrogenation, Nat. Commun. 10 (2019) 4012, https://doi.org/10.1038/s41467-019-11940-0.
[107] P. Botella, J.M. López Nieto, B. Solsona, A. Mifsud, F. Márquez, The Preparation, Characterization, and Catalytic Behavior of MoVTeNbO Catalysts Prepared by Hydrothermal Synthesis, J. Catal. 209 (2002) 445–455, https://doi.org/10.1006/jcat.2002.3648.
[108] R. Schlögl, Active Sites for Propane Oxidation: Some Generic Considerations, Top. Catal. 54 (2011) 627–638, https://doi.org/10.1007/s11244-011-9683-0.
[109] Mestl, G.; Wanniger, K.; Melzer, D.; Sanchez-Sanchez, M.C.; Tseglakova, J.; Lercher, J. Synthesis of a MoVNbTe Catalyst Having a Reduced Niobium and Tellurium Content and Higher Activity for the Oxidative Dehydrogenation of Ethane. WO2018141652A1, (n.d.).
[110] F. Ivars, B. Solsona, S. Hernández, J.M.L.ópez Nieto, Influence of gel composition in the synthesis of MoVTeNb catalysts over their catalytic performance in partial propane and propylene oxidation, Catal. Today 149 (2010) 260–266, https://doi.org/10.1016/j.cattod.2009.09.018.
[111] N.R. Shiju, X. Liang, A.W. Weimer, C. Liang, S. Dai, V.V. Guliants, The Role of Surface Basal Planes of Layered Mixed Metal Oxides in Selective Transformation of Lower Alkanes: Propane Ammoxidation over Surface ab Planes of Mo−V−Te−Nb−O M1 Phase, J. Am. Chem. Soc. 130 (2008) 5850–5851, https://doi.org/10.1021/ja800575v.
[112] K. Shimoda, S. Ishikawa, K. Shimizu, W. Ueda, Effects of Local Structural Changes of Orthorhombic Mo3VOx Induced by High-Temperature Heat Treatment on Catalytic Ammoxidation of Propane, ACS Catal. 14 (2024) 13303–13313, https://doi.org/10.1021/acscatal.4c02923.
[113] J.S. Valente, H. Armedáriz-Herrera, R. Quintana-Solórzano, C. Angeles-Chavez, A. Rodríguez-Hernández, M.L. Guzmán-Castillo, J.M. López Nieto, T. Mhin Nha Le, J.-M.M. Millet, Pathway to defective highly active and stable MoVSbOx

catalysts for ethane oxidative dehydrogenation through a dislodging process involving controlled combustion of amino-organic compounds, J. Catal. 427 (2023) 115106, https://doi.org/10.1016/j.jcat.2023.115106.
[114] M.M. Lin, Complex metal oxide catalysts for selective oxidation of propane and derivatives, Appl. Catal. A Gen. 250 (2003) 287–303, https://doi.org/10.1016/S0926-860X(03)00256-4.
[115] J. Oliver, The effect of pH on structural and catalytic properties of MoVTeNbO catalysts, Appl. Catal. A Gen. 257 (2004) 67–76, https://doi.org/10.1016/S0926-860X(03)00632-X.
[116] P. DeSanto, D.J. Buttrey, R.K. Grasselli, C.G. Lugmair, A.F. Volpe, B.H. Toby, T. Vogt, Structural aspects of the M1 and M2 phases in MoVNbTeO propane ammoxidation catalysts, Z. Krist. Cryst. Mater. 219 (2004) 152–165, https://doi.org/10.1524/zkri.219.3.152.29091.
[117] L. Annamalai, Y. Liu, S. Ezenwa, Y. Dang, S.L. Suib, P. Deshlahra, Influence of Tight Confinement on Selective Oxidative Dehydrogenation of Ethane on MoVTeNb Mixed Oxides, ACS Catal. 8 (2018) 7051–7067, https://doi.org/10.1021/acscatal.8b01586.
[118] P. Concepción, S. Hernández, J.M.L. Nieto, On the nature of active sites in MoVTeO and MoVTeNbO catalysts: The influence of catalyst activation temperature, Appl. Catal. A Gen. 391 (2011) 92–101, https://doi.org/10.1016/j.apcata.2010.05.011.
[119] R.K. Grasselli, J.D. Burrington, D.J. Buttrey, P. Desanto, C.G. Lugmair, A.F. Volpe, T. Weingand, Multifunctionality of Active Centers in (Amm)oxidation Catalysts: From Bi–Mo–Ox to Mo–V–Nb–(Te, Sb)–Ox, Top. Catal. 23 (2003) 5–22, https://doi.org/10.1023/A:1024859917786.
[120] R.K. Grasselli, D.J. Buttrey, P. DeSanto, J.D. Burrington, C.G. Lugmair, A.F. Volpe, T. Weingand, Active centers in Mo–V–Nb–Te–Ox (amm)oxidation catalysts, Catal. Today 91– 92 (2004) 251–258, https://doi.org/10.1016/j.cattod.2004.03.060.
[121] M. Aouine, J.M.M. Millet, J.L. Dubois, Crystal chemistry and phase composition of the MoVTeNbO catalysts for the ammoxidation of propane, Chem. Commun. (2001) 1180–1181, https://doi.org/10.1039/b103895h.
[122] J.M.M. Millet, M. Baca, A. Pigamo, D. Vitry, W. Ueda, J.L. Dubois, Study of the valence state and coordination of antimony in MoVSbO catalysts determined by XANES and EXAFS, Appl. Catal. A Gen. 244 (2003) 359–370, https://doi.org/10.1016/S0926-860X(02)00614-2.
[123] Y. Zhu, P.V. Sushko, D. Melzer, E. Jensen, L. Kovarik, C. Ophus, M. Sanchez-Sanchez, J.A. Lercher, N.D. Browning, Formation of Oxygen Radical Sites on MoVNbTeOx by Cooperative Electron Redistribution, J. Am. Chem. Soc. 139 (2017) 12342–12345, https://doi.org/10.1021/jacs.7b05240.
[124] D. Melzer, P. Xu, D. Hartmann, Y. Zhu, N.D. Browning, M. Sanchez-Sanchez, J. A. Lercher, Atomic-Scale Determination of Active Facets on the MoVTeNb Oxide M1 Phase and Their Intrinsic Catalytic Activity for Ethane Oxidative Dehydrogenation, Angew. Chem., Int. Ed. 55 (2016) 8873–8877, https://doi.org/10.1002/anie.201600463.
[125] C. Heine, M. Hävecker, A. Trunschke, R. Schlögl, M. Eichelbaum, The impact of steam on the electronic structure of the selective propane oxidation catalyst MoVTeNb oxide (orthorhombic M1 phase, Phys. Chem. Chem. Phys. 17 (2015) 8983–8993, https://doi.org/10.1039/C5CP00289C.
[126] X. Yang, R. Feng, W. Ji, C. Au, Characterization and evaluation of MoVTeNb mixed metal oxide catalysts fabricated via hydrothermal process with ultrasonic pretreatment for propane partial oxidation, J. Catal. 253 (2008) 57–65, https://doi.org/10.1016/j.jcat.2007.10.020.
[127] R.K. Grasselli, D.J. Buttrey, J.D. Burrington, A. Andersson, J. Holmberg, W. Ueda, J. Kubo, C.G. Lugmair, A.F. Volpe, Active centers, catalytic behavior, symbiosis and redox properties of MoV(Nb,Ta)TeO ammoxidation catalysts, Top. Catal. 38 (2006) 7–16, https://doi.org/10.1007/s11244-006-0066-x.
[128] T. Vogt, D.A. Blom, L. Jones, D.J. Buttrey, ADF-STEM Imaging of Nascent Phases and Extended Disorder Within the Mo–V–Nb–Te–O Catalyst System, Top. Cata. l 59 (2016) 1489–1495, https://doi.org/10.1007/s11244-016-0665-0.
[129] D.A. Blom, T. Vogt, L.F. Allard, D.J. Buttrey, Observation of Sublattice Disordering of the Catalytic Sites in a Complex Mo–V–Nb–Te–O Oxidation Catalyst Using High Temperature STEM Imaging, Top. Catal. 57 (2014) 1138–1144, https://doi.org/10.1007/s11244-014-0278-4.
[130] H. Murayama, D. Vitry, W. Ueda, G. Fuchs, M. Anne, J.L. Dubois, Structure characterization of orthorhombic phase in MoVTeNbO catalyst by powder X-ray diffraction and XANES, Appl. Catal. A Gen. 318 (2007) 137–142, https://doi.org/10.1016/j.apcata.2006.10.050.
[131] A. Govindasamy, K. Muthukumar, J. Yu, Y. Xu, V.V. Guliants, Adsorption of Propane, Isopropyl, and Hydrogen on Cluster Models of the M1 Phase of Mo−V−Te−Nb−O Mixed Metal Oxide Catalyst, J. Phys. Chem. C. 114 (2010) 4544–4549, https://doi.org/10.1021/jp910382x.
[132] X. Li, D.J. Buttrey, D.A. Blom, T. Vogt, Improvement of the Structural Model for the M1 Phase Mo–V–Nb–Te–O Propane (Amm)oxidation Catalyst, Top. Catal. 54 (2011) 614–626, https://doi.org/10.1007/s11244-011-9684-z.
[133] G. Fu, X. Xu, P. Sautet, Vanadium Distribution in Four-Component Mo-V-Te-Nb Mixed-Oxide Catalysts from First Principles: How to Explore the Numerous Configurations? Angew. Chem. Inter. Ed. 51 (2012) 12854–12858, https://doi.org/10.1002/anie.201207638.
[134] P. Korovchenko, N.R. Shiju, A.K. Dozier, U.M. Graham, M.O. Guerrero-Pérez, V. V. Guliants, M1 to M2 Phase Transformation and Phase Cooperation in Bulk Mixed Metal Mo–V–M–O (M=Te, Nb) Catalysts for Selective Ammoxidation of Propane, Top. Catal. 50 (2008) 43–51, https://doi.org/10.1007/s11244-008-9098-8.
[135] M. Baca, M. Aouine, J.L. Dubois, J.M.M. Millet, Synergetic effect between phases in MoVTe(Sb)NbO catalysts used for the oxidation of propane into acrylic acid, J. Catal. 233 (2005) 234–241, https://doi.org/10.1016/j.jcat.2004.12.002.
[136] T. Konya, T. Katou, T. Murayama, S. Ishikawa, M. Sadakane, D. Buttrey, W. Ueda, An orthorhombic Mo3VOx catalyst most active for oxidative dehydrogenation of ethane among related complex metal oxides, Catal. Sci. Technol. 3 (2013) 380–387, https://doi.org/10.1039/C2CY20444D.
[137] O.V. Safonova, B. Deniau, J.-M.M. Millet, Mechanism of the Oxidation−Reduction of the MoVSbNbO Catalyst: In Operando X-ray Absorption Spectroscopy and Electrical Conductivity Measurements, J. Phys. Chem. B 110 (2006) 23962–23967, https://doi.org/10.1021/jp064347l.
[138] Y. Chen, S. Qian, K. Feng, Z. Li, B. Yan, Y. Cheng, Determination of highly active and selective surface for the oxidative dehydrogenation of ethane over phase-pure M1 MoVNbTeOx catalyst, J. Catal. 416 (2022) 277–288, https://doi.org/10.1016/j.jcat.2022.11.011.
[139] M. Baca, J.-M.M. Millet, Bulk oxidation state of the different cationic elements in the MoVTe(Sb)NbO catalysts for oxidation or ammoxidation of propane, Appl. Catal. A Gen. 279 (2005) 67–77, https://doi.org/10.1016/j.apcata.2004.10.014.
[140] N.R. Shiju, A.J. Rondinone, D.R. Mullins, V. Schwartz, S.H. Overbury, V. V. Guliants, XANES Study of Hydrothermal Mo-V-Based Mixed Oxide M1-Phase Catalysts for the (Amm)oxidation of Propane, Chem. Mater. 20 (2008) 6611–6616, https://doi.org/10.1021/cm800546h.
[141] B. Deniau, T.T. Nguyen, P. Delichere, O. Safonova, J.-M.M. Millet, Redox State Dynamics at the Surface of MoVTe(Sb)NbO M1 Phase in Selective Oxidation of Light Alkanes, Top. Catal. 56 (2013) 1952–1962, https://doi.org/10.1007/s11244-013-0132-0.
[142] M. Aouine, T. Epicier, J.-M.M. Millet, In Situ Environmental STEM Study of the MoVTe Oxide M1 Phase Catalysts for Ethane Oxidative Dehydrogenation, ACS Catal. 6 (2016) 4775–4781, https://doi.org/10.1021/acscatal.6b01114.
[143] D. Melzer, G. Mestl, K. Wanninger, A. Jentys, M. Sanchez-Sanchez, J.A. Lercher, On the Promoting Effects of Te and Nb in the Activity and Selectivity of M1 MoV-Oxides for Ethane Oxidative Dehydrogenation, Top. Catal. 63 (2020) 1754–1764, https://doi.org/10.1007/s11244-020-01304-0.
[144] G.Ya Popova, T.V. Andrushkevich, Yu.A. Chesalov, L.M. Plyasova, L.S. Dovlitova, E.V. Ischenko, G.I. Aleshina, M.I. Khramov, Formation of active phases in MoVTeNb oxide catalysts for ammoxidation of propane, Catal. Today 144 (2009) 312–317, https://doi.org/10.1016/j.cattod.2009.01.049.
[145] P. Kube, B. Frank, S. Wrabetz, J. Kröhnert, M. Hävecker, J. Velasco-Vélez, J. Noack, R. Schlögl, A. Trunschke, Functional Analysis of Catalysts for Lower Alkane Oxidation, ChemCatChem 9 (2017) 573–585, https://doi.org/10.1002/cctc.201601194.
[146] I. Ramli, P. Botella, F. Ivars, W. Pei Meng, S.M.M. Zawawi, H.A. Ahangar, S. Hernández, J.M.L. Nieto, Reflux method as a novel route for the synthesis of MoVTeNbOx catalysts for selective oxidation of propane to acrylic acid, J. Mol. Catal. A Chem. 342–343 (2011) 50–57, https://doi.org/10.1016/j.molcata.2011.04.009.
[147] Y.S. Yun, M. Lee, J. Sung, D. Yun, T.Y. Kim, H. Park, K.R. Lee, C.K. Song, Y. Kim, J. Lee, Y.-J. Seo, I.K. Song, J. Yi, Promoting effect of cerium on MoVTeNb mixed oxide catalyst for oxidative dehydrogenation of ethane to ethylene, Appl. Catal. B 237 (2018) 554–562, https://doi.org/10.1016/j.apcatb.2018.06.025.
[148] A. de Arriba, B. Solsona, A.M. Dejoz, P. Concepción, N. Homs, P.R. de la Piscina, J.M.L.ópez Nieto, Evolution of the optimal catalytic systems for the oxidative dehydrogenation of ethane: The role of adsorption in the catalytic performance, J. Catal. 408 (2022) 388–400, https://doi.org/10.1016/j.jcat.2021.07.015.
[149] E.V. Ishchenko, T.V. Andrushkevich, G.Ya Popova, T.Yu Kardash, A.V. Ishchenko, L.S. Dovlitova, Yu.A. Chesalov, The structure and catalytic properties of amorphous phase in MoVTeO catalysts for propane ammoxidation, Appl. Catal. A Gen. 476 (2014) 91–102, https://doi.org/10.1016/j.apcata.2014.02.022.
[150] L. Yuan, V.V. Guliants, M.A. Bañares, S.J. Khatib, TIC-09-Mesoporous Niobium-Based Mixed Metal Oxides Containing Mo, V, and Te for Propane Oxidative Dehydrogenation, Top. Catal. 49 (2008) 268–280, https://doi.org/10.1007/s11244-008-9085-0.
[151] V.V. Guliants, H.H. Brongersma, A. Knoester, A.M. Gaffney, S. Han, Surface active sites present in the orthorhombic M1 phases: low energy ion scattering study of methanol and allyl alcohol chemisorption over Mo–V–Te–Nb–O and Mo–V–O catalysts, Top. Catal. 38 (2006) 41–50, https://doi.org/10.1007/s11244-006-0069-7.
[152] V.V. Guliants, R. Bhandari, A.R. Hughett, S. Bhatt, B.D. Schuler, H.H. Brongersma, A. Knoester, A.M. Gaffney, S. Han, Probe Molecule Chemisorption−Low Energy Ion Scattering Study of Surface Active Sites Present in the Orthorhombic Mo−V−(Te−Nb)−O Catalysts for Propane (Amm)oxidation, J. Phys. Chem. B 110 (2006) 6129–6140, https://doi.org/10.1021/jp056720f.
[153] A. Celaya Sanfiz, T.W. Hansen, A. Sakthivel, A. Trunschke, R. Schlögl, A. Knoester, H.H. Brongersma, M.H. Looi, S.B.A. Hamid, How important is the (001) plane of M1 for selective oxidation of propane to acrylic acid? J. Catal. 258 (2008) 35–43, https://doi.org/10.1016/j.jcat.2008.05.028.
[154] W. Ueda, D. Vitry, T. Katou, Structural organization of catalytic functions in Mo-based oxides for propane selective oxidation, Catal. Today 96 (2004) 235–240, https://doi.org/10.1016/j.cattod.2004.06.147.
[155] A.C. Sanfiz, T.W. Hansen, D. Teschner, P. Schnörch, F. Girgsdies, A. Trunschke, R. Schlögl, M.H. Looi, S.B.A. Hamid, Dynamics of the MoVTeNb Oxide M1 Phase in Propane Oxidation, J. Phys. Chem. C. 114 (2010) 1912–1921, https://doi.org/10.1021/jp909352u.
[156] J.S. Valente, R. Quintana-Solórzano, H. Armendáriz-Herrera, G. Barragán-Rodríguez, J.M. López-Nieto, Kinetic Study of Oxidative Dehydrogenation of Ethane over MoVTeNb Mixed-Oxide Catalyst, Ind. Eng. Chem. Res. 53 (2014) 1775–1786, https://doi.org/10.1021/ie402447h.

[157] P. Botella, J.M. López Nieto, A. Dejoz, M.I. Vázquez, A. Martínez-Arias, Mo–V–Nb mixed oxides as catalysts in the selective oxidation of ethane, Catal. Today 78 (2003) 507–512, https://doi.org/10.1016/S0920-5861(02)00338-3.
[158] M. Merzouki, B. Taouk, L. Tessier, E. Bordes, P. Courtine, Correlation Between Catalytic and Structural Properties of Modified Molybdenum and Vanadium Oxides in the Oxidation of Ethane in Acetic Acid or Ethylene, in: 1993: pp. 753–764. https://doi.org/10.1016/S0167-2991(08)64054-9.
[159] K. Ruth, R. Burch, R. Kieffer, Mo–V–Nb Oxide Catalysts for the Partial Oxidation of Ethane, J. Catal. 175 (1998) 27–39, https://doi.org/10.1006/jcat.1998.1976.
[160] K. Ruth, R. Kieffer, R. Burch, Mo–V–Nb Oxide Catalysts for the Partial Oxidation of Ethane, J. Catal. 175 (1998) 16–26, https://doi.org/10.1006/jcat.1998.1975.
[161] Y.V. Kolen'ko, W. Zhang, R.N. D'Alnoncourt, F. Girgsdies, T.W. Hansen, T. Wolfram, R. Schlögl, A. Trunschke, Synthesis of MoVTeNb Oxide Catalysts with Tunable Particle Dimensions, ChemCatChem 3 (2011) 1597–1606, https://doi.org/10.1002/cctc.201100089.
[162] V.V. Guliants, R. Bhandari, H.H. Brongersma, A. Knoester, A.M. Gaffney, S. Han, A Study of the Surface Region of the Mo−V−Te−O Catalysts for Propane Oxidation to Acrylic Acid, J. Phys. Chem. B 109 (2005) 10234–10242, https://doi.org/10.1021/jp044120v.
[163] A. Trunschke, J. Noack, S. Trojanov, F. Girgsdies, T. Lunkenbein, V. Pfeifer, M. Hävecker, P. Kube, C. Sprung, F. Rosowski, R. Schlögl, The Impact of the Bulk Structure on Surface Dynamics of Complex Mo–V-based Oxide Catalysts, ACS Catal. 7 (2017) 3061–3071, https://doi.org/10.1021/acscatal.7b00130.
[164] V.V. Guliants, R. Bhandari, B. Swaminathan, V.K. Vasudevan, H.H. Brongersma, A. Knoester, A.M. Gaffney, S. Han, Roles of Surface Te, Nb, and Sb Oxides in Propane Oxidation to Acrylic Acid over Bulk Orthorhombic Mo−V−O Phase, J. Phys. Chem. B 109 (2005) 24046–24055, https://doi.org/10.1021/jp054641y.
[165] R. Burch, R. Swarnakar, Oxidative dehydrogenation of ethane on vanadium-molybdenum oxide and vanadium-niobium-molybdenum oxide catalysts, Appl. Catal. 70 (1991) 129–148, https://doi.org/10.1016/S0166-9834(00)84159-7.
[166] Y. Chen, D. Dang, B. Yan, Y. Cheng, Nanocomposite catalysts of non-purified MoVNbTeOx with CeO2 or TiO2 for oxidative dehydrogenation of ethane, Chem. Eng. Sci. 264 (2022) 118154, https://doi.org/10.1016/j.ces.2022.118154.
[167] D.A. Svintsitskiy, T.Yu Kardash, E.V. Lazareva, A.A. Saraev, E.A. Derevyannikova, M. Vorokhta, B. Šmíd, V.M. Bondareva, NAP-XPS and in situ XRD study of the stability of Bi-modified MoVNbTeO catalysts for oxidative dehydrogenation of ethane, Appl. Catal. A Gen. 579 (2019) 141–150, https://doi.org/10.1016/j.apcata.2019.04.027.
[168] J.S. Valente, E. Maya-Flores, H. Armendáriz-Herrera, R. Quintana-Solórzano, J.M. L.ópez Nieto, Metal solution precursors: their role during the synthesis of MoVTeNb mixed oxide catalysts, Catal. Sci. Technol. 8 (2018) 3123–3132, https://doi.org/10.1039/C8CY00750K.
[169] M. Sanchez Sanchez, F. Girgsdies, M. Jastak, P. Kube, R. Schlögl, A. Trunschke, Aiding the Self-Assembly of Supramolecular Polyoxometalates under Hydrothermal Conditions To Give Precursors of Complex Functional Oxides, Angew. Chem. Inter. Ed. 51 (2012) 7194–7197, https://doi.org/10.1002/anie.201200746.
[170] Y. Suchorski, L. Rihko-Struckmann, F. Klose, Y. Ye, M. Alandjiyska, K. Sundmacher, H. Weiss, Evolution of oxidation states in vanadium-based catalysts under conventional XPS conditions, Appl. Surf. Sci. 249 (2005) 231–237, https://doi.org/10.1016/j.apsusc.2004.11.083.
[171] C. Rameshan, H. Li, K. Anic, M. Roiaz, V. Pramhaas, R. Rameshan, R. Blume, M. Hävecker, J. Knudsen, A. Knop-Gericke, G. Rupprechter, In situ NAP-XPS spectroscopy during methane dry reforming on ZrO2/Pt(1, 1 1) Inverse Model Catal., J. Phys.: Condens. Matter 30 (2018) 264007, https://doi.org/10.1088/1361-648X/aac6ff.
[172] A.M. Gaffney, Q. An, W.A. Goddard, W. Diao, M.V. Glazoff, Toward Concurrent Engineering of the M1-Based Catalytic Systems for Oxidative Dehydrogenation (ODH) of Alkanes, Top. Catal. 63 (2020) 1667–1681, https://doi.org/10.1007/s11244-020-01327-7.
[173] Y. Chen, B. Yan, Y. Cheng, State-of-the-Art Review of Oxidative Dehydrogenation of Ethane to Ethylene over MoVNbTeOx Catalysts, Catalysts 13 (2023) 204, https://doi.org/10.3390/catal13010204.
[174] G. Che-Galicia, R.S. Ruiz-Martínez, F. López-Isunza, C.O. Castillo-Araiza, Modeling of oxidative dehydrogenation of ethane to ethylene on a MoVTeNbO/TiO2 catalyst in an industrial-scale packed bed catalytic reactor, Chem. Eng. J. 280 (2015) 682–694, https://doi.org/10.1016/j.cej.2015.05.128.
[175] R. Quintana-Solórzano, G. Barragán-Rodríguez, H. Armendáriz-Herrera, J. M. López-Nieto, J.S. Valente, Understanding the kinetic behavior of a Mo–V–Te–Nb mixed oxide in the oxydehydrogenation of ethane, Fuel 138 (2014) 15–26, https://doi.org/10.1016/j.fuel.2014.07.051.
[176] G. Che-Galicia, R. Quintana-Solórzano, R.S. Ruiz-Martínez, J.S. Valente, C. O. Castillo-Araiza, Kinetic modeling of the oxidative dehydrogenation of ethane to ethylene over a MoVTeNbO catalytic system, Chem. Eng. J. 252 (2014) 75–88, https://doi.org/10.1016/j.cej.2014.04.042.
[177] P.J. Donaubauer, D.M. Melzer, K. Wanninger, G. Mestl, M. Sanchez-Sanchez, J. A. Lercher, O. Hinrichsen, Intrinsic kinetic model for oxidative dehydrogenation of ethane over MoVTeNb mixed metal oxides: A mechanistic approach, Chem. Eng. J. 383 (2020) 123195, https://doi.org/10.1016/j.cej.2019.123195.
[178] M. Merzouki, B. Taouk, L. Monceaux, E. Bordes, P. Courtine, Catalytic Properties Of Promoted Vanadium Oxide In The Oxidation Of Ethane In Acetic Acid, in: 1992: pp. 165–179. https://doi.org/10.1016/S0167-2991(08)61669-9.
[179] Y. Liu, L. Annamalai, P. Deshlahra, Effects of Lattice O Atom Coordination and Pore Confinement on Selectivity Limitations for Ethane Oxidative Dehydrogenation Catalyzed by Vanadium-Oxo Species, J. Phys. Chem. C. 123 (2019) 28168–28191, https://doi.org/10.1021/acs.jpcc.9b07778.
[180] E.V. Ishchenko, R.V. Gulyaev, T.Yu Kardash, A.V. Ishchenko, E.Yu Gerasimov, V. I. Sobolev, V.M. Bondareva, Effect of Bi on catalytic performance and stability of MoVTeNbO catalysts in oxidative dehydrogenation of ethane, Appl. Catal. A Gen. 534 (2017) 58–69, https://doi.org/10.1016/j.apcata.2017.01.023.
[181] E.V. Ishchenko, T.Yu Kardash, R.V. Gulyaev, A.V. Ishchenko, V.I. Sobolev, V. M. Bondareva, Effect of K and Bi doping on the M1 phase in MoVTeNbO catalysts for ethane oxidative conversion to ethylene, Appl. Catal. A Gen. 514 (2016) 1–13, https://doi.org/10.1016/j.apcata.2015.12.018.
[182] E.V. Lazareva, V.M. Bondareva, D.A. Svintsitskiy, A.V. Ishchenko, A.S. Marchuk, E.P. Kovalev, T.Yu Kardash, Oxidative dehydrogenation of ethane over M1 MoVNbTeO catalysts modified by the addition of Nd, Mn, Ga or Ge, Catal. Today 361 (2021) 50–56, https://doi.org/10.1016/j.cattod.2019.12.029.